January 2018

Effect Of Cisplatin On Metallothionein Expression In Urotsa Cells Malignantly Transformed With Arsenite Or Cadmium

Brooke Alexandra Freeberg

Follow this and additional works at: https://commons.und.edu/theses

EFFECT OF CISPLATIN ON METALLOTHIONEIN EXPRESSION IN UROTSA CELLS MALIGNANTLY TRANSFORMED WITH ARSENITE OR CADMIUM

by

Brooke Alexandra Freeberg
Bachelor of Science, University of North Dakota, 2016

A Thesis
Submitted to the Graduate Faculty

of the

University of North Dakota
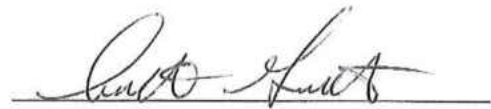
in partial fulfillment of requirements
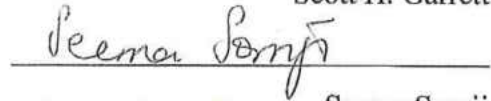

for the degree of

Masters of Science

Grand Forks, North Dakota
December
2018
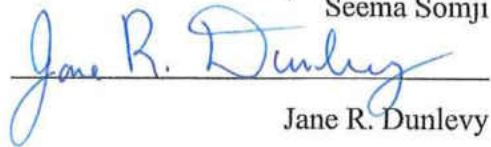
This thesis, submitted by Brooke Alexandra Freeberg in partial fulfillment of the requirements for the degree of Masters of Science from the University of North Dakota, has been read by the Faculty Advisory Committee under whom the work has been done and is hereby approved.

_____

Scott H. Garrett

_____

Seema Somji

_____

Jane R. Dunlevy

This thesis is being submitted by the appointed advisory committee as having met all of the requirements of the School of Graduate Studies at the University of North Dakota and is hereby approved.

_____

Grant McGimpsey
Dean of the School of Graduate Studies

December 6, 2018

Date

PERMISSION.

Title   EFFECT OF CISPLATIN ON METALLOTHIONEIN EXPRESSION IN
UROTSA CELLS MALIGNANTLY TRANSFORMED WITH ARSENITE
OR CADMIUM

Department   Pathology

Degree   Masters of Science

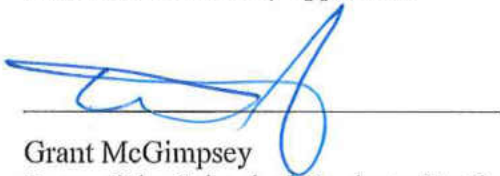In presenting this thesis in partial fulfillment of the requirements for a graduate degree from the University of North Dakota, I agree that the library of this University shall make it freely available for inspection. I further agree that permission for extensive copying for scholarly purposes may be granted by the professor who supervised my thesis work or, in her absence, by the Chairperson of the department or the dean of the School of Graduate Studies. It is understood that any copying or publication or other use of this thesis or part thereof for financial gain shall not be allowed without my written permission. It is also understood that due recognition shall be given to me and to the University of North Dakota in any scholarly use which may be made of any material in my thesis.

<div align="right">
Brooke Alexandra Freeberg
November 19, 2018
</div>

TABLE OF CONTENTS.

CHAPTERS.

LIST OF FIGURES.

LIST OF TABLES.

ACKNOWLEDGEMENTS.

I would also like to thank my husband Aaron Dolby for putting up with me. Thank you for dealing with me when I was stressed or upset with never-ending trips for ice cream and French fries to cheer me up. It means a lot that you have stood by my side through everything and will continue to stand by my side through life.

Lastly, I am thankful for the immeasurable support from my family. Lauren, thank you for letting me invade your apartment for frequent sister dinners. Paige, thank you for your never-ending support and cheering me on from a distance. Mama and Dad, thank you for always pushing me to be the best version of myself and for always having my back. This degree would not have been possible without your constant inspiration and sacrifices for my future.

To my parents, Troy and Wendy Freeberg, and to my husband, Aaron Dolby.
Thank you for being the people you are and making me into the best version of myself.
This is possible due to your support.

ABSTRACT.

Heavy metals Arsenite (As^{3+}) and Cadmium (Cd^{2+}) are known human carcinogens and exposure to them occurs through cigarette smoking, industrialization, and contaminated water sources. Epidemiological studies have shown that prolonged exposure to these heavy metals are associated with several health issues, including bladder cancer. With survival rates directly correlated to detection age and tumor stage, the demand for early detection would effectively cut costs and improve the patient prognosis of human bladder cancer.

Metallothioneins (MT) play an essential role in metal regulation, heavy metal detoxification, and cellular redox chemistry in cellular biological systems and tissues. Previous studies in literature have found elevated MT expression in patients with kidney, breast, prostate and bladder cancers. This increased presence of MT may contribute to the resistance to the chemotherapy drug Cis-diamminediechloroplatinum(II), CDDP (Cisplatin) in human bladder cancer.

Previous studies from our laboratory have shown that As^{3+} and Cd^{2+} can malignantly transform the human urothelial cell line UROtsa and these transformed cells can form subcutaneous, as well as, intraperitoneal tumors. The first goal of this study is

to determine the expression level of six MT isoforms (MT-1A, MT-1E, MT-1F, MT-1X, MT-2A, and MT-3) in the Parent UROtsa cell line and the 13 independently derived As^{+3}-and Cd^{+2}-transformed cell lines. The second goal of this study is to determine the expression levels of the same six MT isoforms in the Parent UROtsa and in two As^{+3} (As #1 and As #5) -and two Cd^{+2} (Cd #1 and Cd #4) -transformed cell lines when they were acutely exposed to various concentrations of the chemotherapy drug, cisplatin.

For this study, Messenger Ribonucleic Acid (mRNA) was isolated from the Parent UROtsa cell line and the 13 independently derived As^{+3}-and Cd^{+2}-transformed cell lines, as well as, two As^{+3} (As #1 and As #5) -and two Cd^{+2} (Cd #1 and Cd #4) -transformed cell lines and the Parent UROtsa after the cells were acutely exposed to cisplatin. Real Time Reverse Transcriptase Quantitative Polymerase Chain Reaction (RT-qPCR) was performed to determine the basal expression of the six MT isoforms in the Parent UROtsa cell line and the 13 independently derived As^{+3}-and Cd^{+2}-transformed cell lines. Real Time RT-qPCR was also performed to determine the corresponding expression of the Parent UROtsa and in two As^{+3} -and two Cd^{+2} -transformed cell lines after the cells were acutely exposed to cisplatin. The results demonstrated an overall decrease in the expression of the six MT isoforms in the transformed cell lines compared to the Parent UROtsa, as well as, an overall decrease in expression after exposure to cisplatin when compared to the basal expression levels.

In order to further look at the basal expression, Immunohistochemical (IHC) analysis was performed on the subcutaneous transplants generated by the subcutaneous injection of the 13 independently derived As^{+3}-and Cd^{+2}-transformed cell lines into immune compromised mice. The six As^{3+} and the seven Cd^{2+} UROtsa mouse

subcutaneous tumors were stained for MT isoforms 1/2 and MT isoform 3. MT isoforms 1/2 staining of the 13 UROtsa mouse subcutaneous tumors show moderate or weak-to-moderate staining. MT isoform 3 showed strong and diffuse staining, however the peripheral less differentiated tumor cells showed weaker staining.

Additionally, western blot analysis was performed to determine the levels of MT proteins in the Parent UROtsa and two of the As^{3+} -and two of the Cd^{2+} -transformed cell lines. Overall, the results demonstrated a decrease in the levels of total MT in the Parent UROtsa, as well as, the transformed cell lines.

In conclusion, our data shows that exposure to As^{3+} or Cd^{2+} decreases the expression of the six MT isoforms. This decrease in MT expression may disrupt the normal cellular redox within the cells, thus promoting the transformation process. In addition, exposure to cisplatin demonstrated a decrease in expression of the six MT isoforms, which may have implications in the treatment of human bladder cancer with this drug.

CHAPTER I.

INTRODUCTION.

The Human Urinary System.

The human urinary system is made up of organs, tubes, and muscles that regulate and eliminate toxic chemicals from the body using paired kidneys, paired ureters, urinary bladder, and urethra as the primary components (Zimmermann, 2018). To maintain homeostasis the body relays the urinary system for filtration and excretion of urine (Ross & Pawlina, 2016).

The human urinary bladder is a distensible reservoir for urine that is located in the pelvis and maintains three openings, two for the ureters and one for the urethra (Ross & Pawlina, 2016). The urinary bladder has two important functions: storage of urine and emptying of urine (Andersson & Arner, 2004). During urine storage the bladder retains low pressure, which contracts to high pressure during the emptying phase. The detrusor smooth muscle is the main muscle component of the urinary bladder wall (Andersson & Arner,

2004). During the process of urination the sphincters relax allowing urine to pass through the urethra (Urinary Retention, 2018)**.**

On average, adults filter and dispose of about one liter and a half of urine each day, which makes the human bladder a major site for prolonged chemical exposure (Keil, Berger-Ritchie, & McMilin, 2011). Urine retention can produce severe urinary infections, bacterial infections, and even advance into cancer that can affect the entire urinary system (Selius & Subedi, 2008).

Environmental Background of Human Bladder Cancer.

In 1895, the discoveries of Ludwig Rehn initiated the first connection between bladder cancer and environmental agents in Frankfurt, Germany (Rehn, 1895). Rehn was attracted to the increasing prevalence of bladder cancer among workers in German dye manufacturer plants (Dietrich & Dietrich, 2001). His studies initially targeted aniline as a potential source, which sparked the association of bladder cancer cases amongst industry workers. This link established occupational toxicity as a mediator to bladder cancer. Further studies into occupational toxicology exposed carcinogenic aromatic amines found in the production of rubber, textiles, and chemical consequences of industrialization (Johansson & Cohen, 1992). In later years, naphthylamine and aromatic amines were also determined to be cancer-causing agents (Hueper, Wiley, & Wolfe, 1938). Rehn was ultimately responsible for the investigation that lead to regulations to protect workers, which continues to intensify.

Despite robust worker protection laws in 2010 in among men, bladder cancer was still the sixth most common cancer (Jemal, Siegel, Xu, & Ward, 2010). Harmful aromatic amines, unsaturated aldehydes, and Cd^{2+} are known cancer-causing agents that are still present in cigarettes. It is estimated that there is a three times higher risk for bladder cancer in smokers verse non-smokers (Zeegers, Tan, Dorant, & Van Den Brandt, 2000). Smokers are exposed to known cancer-causing agents at a rate of 1.7 µg of Cd^{2+} and 1.4 µg of As^{3+} per cigarette (ATSDR, 2012) (Smith, Livington, & Doolittle, 1997). Elevated and reoccurring exposure to As^{3+} and Cd^{2+} via cigarette smoking is a confirmed risk factor of bladder cancer (Freedman, Silverman, Hollenbeck, Schatzkin, & Abnet, 2011).

Bladder Cancer Prevalence.

Today bladder cancer is the sixth most common cancer in men and the 17th most common cancer in women the United States (Bladder Cancer Statistics, 2018). Bladder cancer is also the tenth most common cancer worldwide (Bladder Cancer Statistics, 2018). In 2014, the Center for Disease Control and Prevention (CDC) estimated 72,462 people (55,014 men and 17,448 women) were living with bladder cancer, and 15,775 (11,291 men and 4,484 women) deaths were due to the disease. Statistically, bladder cancer is more common among Caucasians (whites), and three times more likely in men verse women. The American Cancer Association (ACS) estimates that 9 out of 10 people with bladder cancer are over the age of 55 years old, with the average diagnosis at 73 years old.

The annual cost of bladder cancer was about $4 billion in the United States, when estimated in 2010, and it is predicted to rise to about $5 billion by 2020 (Yeung, Dinh, & Lee, 2014). Bladder cancer poses a significant economic burden due to required lifetime surveillance, treatment for reoccurring tumors, and the overall cost associated with treatment and patient care (Jacobs, Lee, and Montie, 2010).

Over the last decade, several advances have been made in the diagnosis and treatment of human bladder cancer. Research and development continues to strive for expansion of molecular understanding, early detection biomarkers, and improvement of technology such as florescent cystoscopy (Jacobs, Lee, and Montie, 2010).

Arsenite Causes Human Bladder Cancer.

As^{3+} is a metalloid that has both metal, as well as, non-metal properties and has been classified by the International Agency for Research on Cancer (IARC) as a human carcinogen. It has also been evaluated and determined to be hazardous by The Comprehensive Environmental Response, Compensation, and Liability Act, also known as CERCLA. CERCLA's Priority List of Hazardous Substances by the Agency ranked As^{3+} first in 2007 for Toxic Substances and disease Registry (2007 CERCLA Priority List of Hazardous Substances, 2018). Studies show that tens of millions of people are exposed worldwide to As^{3+} and have concluded it is a well-established cause of lung and bladder cancer (Steinmaus, et al., 2014). In addition to lung and bladder cancer, oral ingestion of inorganic As^{3+} is known to cause skin, kidney, liver, and prostate cancer (ATSDR, 2007).

As^{3+}, a ubiquitous metalloid, can exist in both organic and inorganic forms (Mandal & Suzuki, 2002). Organic forms of As^{3+} are associated with carbon (C) and hydrogen (H), while inorganic forms are associated with iron (Fe) , cobalt (Co) or nickel (Ni) coupled with sulfide (S^{2-}) minerals (Bhattacharya, et al., 2007). Inorganic As^{3+} are released into the environment from anthropogenic sources, including both naturally and through human intervened routes. The most notorious exposure routes are metal mining and smelting, pesticide use, wood combustion, as well as, waste combustion (Jang, Somanna, & Kim, 2016) (ASTDR, 2007). As^{3+} released from the soil can be absorbed into ground water. The most common general route of human exposure to As^{3+} is through contaminated drinking water (Chiou, et al., 1995).

Millions of people worldwide are exposed to naturally occurring As^{3+} in their drinking water (Steinmaus, et al., 2013). Bladder cancer was first investigated in Taiwan, as a result to high incidence of Blackfoot disease (BFD) (Tseng, 1997). BFD is a severe form of peripheral vascular disease (PVD), in which the blood vessels in the lower limbs are severely damaged, resulting eventually in progressive gangrene due to As^{3+} exposure (Tseng, et al., 2005). It was most common among farmers in the region tending to their crops (Arsenic, 2018). Studies all around the world have deliberated the effects of As^{3+} in BFD and other various cancers. Many studies have attempted to calculate the maximum containment level (MCL) for the United States that regulates the concentration of As^{3+} that the public is exposed to (Marshall, et al., 2007). As^{3+} has more effects on health than any other toxicant, and the list continues to grow, along with evidence that exposure is widespread throughout the world (Smith & Steinmaus, 2011).

Cadmium Causes Human Bladder Cancer.

Cd^{2+} is a heavy metal that has been classified by the IARC as a human carcinogen. Cd^{2+} has also been specifically studied to have an association with the development of human bladder cancer (Siemiatycki, Dewar, & Gerin, 1994). Cd^{2+} is naturally found in the earth's crust and throughout volcanic emissions, as well as, forest fires and other natural phenomena's (Cadmium, 2018). Additionally, lettuce, spinach, potatoes, peanuts, soybeans, and sunflower seeds are very high sources of natural occurring Cd^{2+} (ATSDR, 2012).

National Toxicology Program (NTP) listed that human exposure to Cd^{2+} is mainly through diet, industrial hazards, and cigarette smoking (NTP, 2011). Occupational exposure is very high among smelting, welding, and other various jobs that produce Cd^{2+} powder (NTP, 2011). Man-made application are the main source of toxic Cd^{2+} release in the environment. The estimated Cd^{2+} intake is 0.35 µg/kg/day in males and 0.30 µg/kg/day for females, which is roughly 1:5 over the daily limit by smoking a single cigarette (Choudhury et al., 2001). Cd^{2+} exposure poses a great health risk to humans since the metal is unable to be metabolized into a less toxic form, while also being poorly secreted due to its long half-life (Satarug & Moore, 2004).

 Cd^{2+} accumulation in the tissues was first studied in 1955 in Japan. The outbreak of Itai-Itai Disease connected contaminated rice paddies, which was the main source of food for residents in the area, to Cd^{2+} (Inaba, et al., 2005). The disease translates to "it hurts-it hurts" which is fitting due to renal injury due to tubular and glomerular dysfunction, followed by bone injury consisting of osteoporosis. The toxicity rigorously spread throughout the body in

parallel with severe pain, ultimately leaving the patients bed-ridden (Biggers & Paddock, 2018).

Cd^{2+} was also intensely studies in northeastern Belgium and southeastern Netherlands due to an established correlation between long term emission of Cd^{2+} by Zn smelters and human bladder cancer. Cd^{2+} is an established carcinogen linked to many cancers but the manner by which Cd^{2+} causes each cancer is not fully elucidated yet.

Arsenite and Cadmium Transformed UROtsa Cells.

The UROtsa cell line originated from urothelial cells derived from the left ureter of a 12-year-old girl. After extraction the cells were immortalized with a temperature sensitive Simian Virus 40 (SV40) large tumor-antigen (T-antigen) gene. Commercially available immortalized human bladder cancer-derived cell lines are well characterized but do not allow for initial stages of carcinogenesis to be effusively investigated. The UROtsa cell morphology aligns with primary urothelial cells growing in tightly packed colonies allowing investigation into the preliminary phase of development (Rossi, et al., 2001).

Our laboratory has exposed the immortalized UROtsa cell line to As^{3+} or Cd^{2+} in order to establish an *in-vitro* cell culture model that is representative of the mechanisms involved in early bladder cancer. Our laboratory strategically exposed non-tumorigenic urothelial cell line, UROtsa, to long term As^{3+} or Cd^{2+} with the endpoint goal of the cells able to form colonies in soft agar and form tumors when heterotransplanted into nude mice (Sens, et al., 2004).

During the transformation, the cells were injected into the nude mice to evaluate tumor formation. Nude mice are a laboratory mouse strain with a genetic mutation that causes an inhibited immune system response and are universally recognized as immunocompromised mice. They are the ideal mouse strain for rapidly growing tumor models since they can receive many different types of tissue and/or tumor grafts without mounting a rejection response. Their hairless nature is also ideal because they do not need to be shaved (Inbred & Outbred Nude Mice, 2018).

The histology of the tumors produced features consistent with those of classic transitional-cell carcinoma (TCC) of bladder cancer. The heterotransplant tumors displayed prominent squamous differentiation. Long-term *in-vitro* exposure causes As^{3+} and Cd^{2+} to malignantly transform urothelial cells as indicated by anchorage independent cell growth and tumor formation in nude mice (Sens, et al., 2004).

Metallothioneins.

Through cysteine residues, MT play an important role in detoxification by uptake, transport, and regulation of metals in biological systems (Mididoddi, McGuirt, Sens, Todd, & Sens 1995). In both mice and humans, there are four classes of comparable MT proteins (Garrett, et al., 1999). MT isoform 1, MT isoform 2, MT isoform 3, and finally MT isoform 4, are defined in literature based on sequence and characteristics. MT are a family of cysteine-rich metal binding antioxidant proteins in humans consisting of 10 functional and seven non-functional isoforms. Of the 10 functional there are seven functional MT isoform

8

1's and one functional gene for MT isoform 2, MT isoform 3, and MT isoform 4 respectively (Liu, et. al., 2007). Within the MT isoform 1 there are seven functional isoforms. For this study we choose to examine four (MT-1A, MT-1E, MT-1F, and MT-1X). Within MT isoform 2 there is one function isoform, MT isoform 2A, which was also used throughout this study. MT isoform 3 has one functional isoform that was looked at in this study because it exhibits tissue-specific expression specifically differentiating this isoform from the ubiquitously expressed MT isoform 1 and MT isoform 2.

MT isoform 1 and MT isoform 2 are ubiquitously expressed at high levels, while MT isoform 3 and MT isoform 4 exhibit more restricted tissue specific expression. MT isoform 1 and MT isoform 2 have been extensively studied and are believed to serve an important role in the homeostasis of essential metals such as Zn^{2+} and Cu^{2+} during growth and development. MT isoform 1 and MT isoform 2 are also important in the detoxification of heavy metals, such as Cd^{2+} and Hg^{2+} (Sens, et al., 2000). Typically MT isoform 3 and MT isoform 4 exhibit more restricted tissue specific expression, with the highest distributions classically recognized to localize to the CNS and stratified epithelium, respectively.

MT are localized to the membrane of the Golgi apparatus with the capacity to bind when metal absorption levels are elevated (Chabin-Brion, et al., 2001). MT are most well-known for its binding affinity with zinc (Zn), copper (Cu), selenium (Se), mercury (Hg), and other heavy metals like As^{3+} or Cd^{2+} (Smith, et al., 2006). MT proteins range from 500 to 14000 Da (5- 14 kDa) in size with 61 to 68 amino acids that remain highly conserved primary and secondary structures across the isoforms (Isani & Carpené, 2014).

While the role of MT in cancer development is still largely unknown, their induction due to heavy metals may be a mediator to cisplatin resistance. At the cellular level MT

9

respond to the presence of cisplatin to trap the central platinum (Pt) element (Hagrman, Goodisman, Dabrowiak, & Souid, 2003). The continued presence of cisplatin causes an upregulated levels of MT, glutathione (GSH), and other cellular thiols, which increase the cell's resistance to cisplatin (Hagrman, Goodisman, Dabrowiak, & Souid, 2003). There is currently very little kinetic data evaluating the relationship between cisplatin and MT.

The Chemotherapy Drug Cisplatin.

Figure I-1. The Cisplatin Drug Structure.

Cisplatin is an anti-cancer chemotherapy

drug (Cisplatin, 2018).

Pt: Platinum, Cl: Chlorine, NH_3: Ammonia.
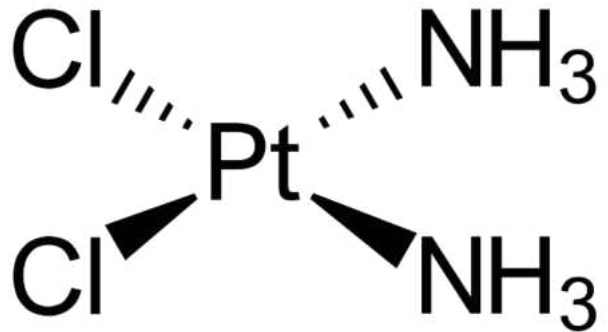
Cisplatin is a small heavy metal complex that reacts with two different sites on Deoxyribonucleic Acid (DNA) leading to the inhibition of synthesis and transcription (Gonzalez, Fuertes, Alonso, & Perez, 2001). Cisplatin, like shown above in Figure I-1, is a central Pt containing anti-cancer drug used to treat not only bladder cancer, but a variety of cancers, including lung, cervical, testicular and ovarian, just to mention a few (Shaloam & Tchounwou, 2015). Unfortunately, this methods it is not always effective since most cancers eventually acquire a resistance to cisplatin following long-term treatment making it a critical target for research. This high probably of developing resistance has a huge medical burden (Oliver, 2010).

Cisplatin is an anti-cancer chemotherapy drug that exerts its antitumor activity by binding to cellular DNA (Gelasco & Lippard, 1998). When cisplatin enters the cell, it passes through the cytosol and crosses the nuclear membrane where it binds to nitrogen (N) atoms on the bases of DNA. When the cisplatin is bound to the DNA it prevents the double helix structure of DNA from linearizing. DNA must be linear into order to be transcribed, therefore cell death is prompted via apoptosis (Ferguson & Baguley, 1994). This ultimately leads to a reduced tumor size as a result of successful treatment with cisplatin.

Statement of Purpose.

Previous studies from our laboratory established that the 13 independently derived As^{+3}-and Cd^{+2}-transformed cell lines are an ideal model system to study TCC or urothelial carcinomas. The first goal of this study is to determine the basal expression level of the six MT isoforms (MT-1A, MT-1E, MT-1F, MT-1X, MT-2A, and MT-3) in the Parent UROtsa and the 13 independently derived As^{+3}-and Cd^{+2}-transformed cell lines. The second goal of this study is to determine the expression levels of the same six MT isoforms in the Parent UROtsa, as well as, two As^{+3} (As #1 and As #5) -and two Cd^{+2} (Cd #1 and Cd #4) -transformed cell lines when they are acutely exposed to various concentrations of the chemotherapy drug, cisplatin. MT are a well-known and highly studied cysteine-rich, low molecular weight family of intracellular proteins that bind to heavy metals with high affinity. MT expression may disrupt the normal cellular redox within the cells, thus promoting the transformation process. In many cancers, there is evidence suggesting that increased expression of MT correlates to cisplatin resistance and poor patient prognosis.

CHAPTER II.

Materials And Methods.

The UROtsa Cell Line Immortalization and Culturing.

The immortalization and culturing of the human urothelial UROtsa cell line was previously described in (Rossi, et al., 2001). In short, the UROtsa cells were maintained at 37.0˚C in a 5.0% carbon dioxide (CO_2) and 95.0% atmosphere oxygen (O). UROtsa cells were grown in 75.0 cm^2 certified cell culture flasks with Dulbecco's Modified Eagle's Medium (DMEM) (Gibco #311320033), supplemented with 5.0% volume-volume percent of fetal calf serum (FCS) (Gibco #10437010). Once the cells reached confluency, the cells were passaged at a 1:3 ratio with 0.25% Trypsin/EDTA, phenol red (Gibco #25200114). Growth media was fed to the cells every three days.

Arsenite and Cadmium Malignant Transformation.

The immortalized urothelial UROtsa cells were malignantly transformed with As^{3+} and Cd^{2+} as previously described in (Sens, et al., 2004). In short, following the identical cell culturing protocol the cells were transformed with 1.0 µM cadmium chloride ($CdCl_2$) (Sigma-Aldrich #7440-23-5), as well as, 1.0 µM sodium arsenite ($NaAsO_2$) (Sigma-Aldrich #S7400-100G). During the transformation, the cells were intermittently tested in order to establish if there was successful colony formation. Colony formation was tested by performing soft agar assays to determine anchorage independent growth. There was six As^{3+} and seven Cd^{2+} isolates were expanded 10 times at a 1:10 ratio before protocol use. The transformed cells were maintained in DMEM supplemented with 5.0% volume-volume percent of FCS and 1.0% glucose. Further subculturing was performed at a 1:10 ratio. All As^{3+} and Cd^{2+} isolates were able to form colonies in soft agar as described in (Sens, et al., 2004).

UROtsa Exposed to Cisplatin Set-up.

The cells were cultured identical to urothelial UROtsa protocol before treatment with cisplatin (Sigma Aldrich #NC0837572). Cisplatin was dissolved in 5.0% molecular grade water (H_2O) and 95.0% sodium chloride (NaCl) prior to sterilization. The stock was further diluted to achieve the desired concentrations with the 1:19 ratio diluent. Cisplatin treatment doses of 0.5 µM and 1.0 µM were added to the cultures when cells

were confluent, and the cells were maintained for Day #1 (24-hours) and Day #2 (48-hours) in 25.0 cm^2 certified cell culture flasks. In order to determine the growth effects of exposure to cisplatin on the Parent UROtsa and two As^{3+} (As #1 and As #5) -and two Cd^{2+} (Cd #1 and Cd #4) -transformed cell lines MTT assays were performed. Cell viability was assessed using 3-(4, 5-Dimethylthiazol-2-yl)-2, 5-diphenyltetrazolium Bromidefor (MTT) assays 3.5 hours after treatment to quantify the cells sensitivity to the cisplatin. Cells were seeded in 6-well plates and allowed to grow for up to six days. Plates of cells were taken daily and exposed to 100.0 mg/mL MTT (Sigma-Aldrich, St. Louis, MO; M5655) for 3.5 hours. Cells were then rinsed twice with phosphate buffered saline and then with 1.0 mL acidic propanol. Optical density was evaluated at 570.0 nm and data was used to calculate doubling times for each cell line. After Day #1 (24-hours) and Day #2 (48-hours), the cells were harvested for protocol use.

Immunohistochemistry Analysis.

Tissue samples were fixed in 10.0 % neutral-buffered formalin for 16 - 18 hours. All tissues were then transferred to 70.0 % ethanol and dehydrated in 100.0 % ethanol. The dehydrated tissues were cleared in xylene, infiltrated, and embedded in paraffin. Serial sections of subcutaneous tumors cut at 3.0 - 5.0 µm were used for IHC. Prior to immunostaining, tissue sections were immersed in preheated Target Retrieval Solution (Dako, Carpinteria, CA) and heated in a steamer for 20.0 minutes. The sections were allowed to cool for 30.0 minutes at room temperature and immersed in TBS-T for 5.0 minutes. The primary antibodies were localized at room temperature for 30.0 minutes

liquid diaminobenzidine (Dako) was used for visualization. Counter staining was

performed for 8.0 minutes at room temperature using Ready-to-use Hematoxylin (Dako).

The major steps are listed below in Table II-1.

Table II-1. Major Steps for Immunohistochemical Staining.	
Target Retrieval Solution	20.0 Minutes
Tris-Buffered Saline with 1.0% Tween	5.0 Minutes
Primary Antibody Incubation	30.0 Minutes
Visualization with 3,3'-Diaminobenzidine (DAB)	10.0 Minutes
Counterstaining with Hematoxylin	8.0 Minutes

The primary antibody used are listed below in Table II-2. Next, the slides were

rinsed with Distilled water, dehydrated in molecular grade ethanol, cleared in xylene

before the coverslip was set. Certified Pathologist at the University of North Dakota

School of Medicine and Health Sciences then examined it.

Table II-2. Antibody used for Immunohistochemistry Analysis.						
Antibody	Dilution	Source & Clonality	Storage	Company	Catalog #	Mw (kDa)
MT, E9	1:200 (BSA)	Mouse Monoclonal	-20°C	DAKO (Agilent)	M0639	6

Protein Isolation.

Total protein was isolated from pellets stored at -80°C. Protein samples were lysed in cold Radioimmunoprecipitation Assay Buffer (RIPA) buffer containing 10.0 µL protease inhibitor, 10.0 µL phenylmethane sulfonyl fluoride (PMSF), and 10.0 µL sodium (Na) orthovanadate (Santa Cruz #24948). Cell pellets were resuspended and incubated on ice for 30.0 minutes on the orbital shaker in the 4°C refrigerator. The extracts were sonicated and then centrifuged at 13,200 relative centrifugal force (rcf) for 10.0 minutes at 4°C. Supernatant was transferred to a cold microfuge tube and the protein concentration was determined through Bicinchoninic Acid Assay (BCA) (Pierce #23228 & #1859078).

For each BCA Assay the dye reagent was prepared by adding 500.0 µL of reagent "B" to 25.0 mL of Reagent "A." The reagents were mixed by inverting the falcon tube several times. Next 2.0 mg/mL of Stock of Albumin Standard (Thermo Fisher #23209) was serial diluted to create standards for the assay. The standards are listed below in Table II-3. The standards created markings for more accurate calculations of the total sample protein concentration. In the 96-well plate 200.0 µL dye and 10.0 µL sample protein was added per well. Once all standards and samples were added the plate was covered with saran wrap and incubated for 30.0 minutes @ 37°C. After incubation the plate absorbance was read at 570.0 nm. The absorbance was then calculated through GraphPad Prism® (Version 7.02) protocol to determine the concentration of the proteins.

Table II-3. BCA Assay Standard Concentrations.			
Tube	Volume of Diluent	Volume of BSA	Final Concentration
A	0.0 µL	300.0 µL of Stock	2,000 µg/mL
B	125.0 µL	375.0 µL of Stock	1,500 µg/mL
C	325.0 µL	325.0 µL of Stock	1,000 µg/mL
D	175.0 µL	175.0 µL of vial B dilution	750 µg/mL
E	325.0 µL	325.0 µL of vial C dilution	500 µg/mL
F	325.0 µL	325.0 µL of vial E dilution	250 µg/mL
G	325.0 µL	325.0 µL of vial F dilution	125 µg/mL
H	400.0 µL	100.0 µL of vial G dilution	25 µg/mL

Real Time Reverse Transcriptase Quantitative Polymerase Chain Reaction.

Total mRNA was isolated from cell pellets using the TRI Reagent® Protocol
(Molecular Research Center, Inc.). mRNA was quantified by spectrophotometry
(Thermo Fisher NanoDrop One). Then 100.0 ng of isolated mRNA was subjected to
complementary DNA (cDNA) synthesis using iScript cDNA Synthesis Kit (BioRad
#170-8891); total volume of 20.0 µL. Real Time RT-qPCR was performed using 10.0 ng
of cDNA with iTag Universal SYBR Green Supermix (BioRad #172-5124). Then 0.2
µM primers in total volume of 20.0 µL were used in a CFX real-time detection system
(BioRad #CFX96). Amplification was monitored by SYBR green fluoresces and
analyzed by interpolation from a quantitative standard curve created from serial dilutions.

Cycling parameters included a 5.0-minute hot start followed by 40.0 cycles of denaturation at 95˚C (30.0 seconds), annealing at 60˚C (30.0 seconds), and extension at 72˚C (30.0 seconds). Confirmation of dominate double stranded species was demonstrated by appropriate denaturation temperature by melt curve analysis. Primers used are indicated below in Tables II-4 and II-5.

Table II-4. Invitrogen Primer Pairs for Real Time RT-qPCR Analysis.	
MT-1A Product: 219 bp	Upper 5' CTCGAAATGGACCCCAACT
	Lower 5' ATATCTTCGAGCAGGGCTGTC
MT-1E Product: 284 bp	Upper 5' GCTTGTTCGTCTCACTGGTG
	Lower 5' CAGGTTGTGCAGGTTGTTCTA
MT-1F Product: 232 bp	Upper 5' AGTCTCTCCTCGGCTTGC
	Lower 5' ACATCTGGGAGAAAGGTTGTC
MT-1X Product: 151 bp	Upper 5' TCTCCTTGCCTCGAAATGGAC
	Lower 5' GGGCACACTTGGCACAGC
MT-2A Product: 259 bp	Upper 5' CCGACTCTAGCCGCCTCTT
	Lower 5' GTGGAAGTCGCGTTCTTTACA
MT-3 Product: 325 bp	Upper 5' CCGTTCACCGCCTCCAG
	Lower 5' CACCAGCCACACTTCACCACA

Table II-5. Other Primers Used for Real Time RT-qPCR Analysis.		
Gene	**Company**	**Catalog Number**
Beta Actin (β-Actin)	BioRad	qHsaCEP0036280

Statistical Analysis.

Statistical analyses were completed using GraphPad Prism® (Version 7.02). Through this software, separate variance t-tests, one-way analysis of variance (ANOVA) with Tukey or Dunnett's post-hoc tests were performed with 0.05 significance. All real time RT-qPCR results were executed in triplicate and express the standard error of the mean (SEM).

Metallothionein Western Blot Analysis.

For western blot analysis protein lysates were mixed with 2X Laemmli Buffer (BioRad #161-0737) containing 5.0 % beta-mercaptoethanol (β-mercaptoethanol) (BioRad #161-0710) and boiled for 5.0 minutes at 95˚C to reduce and denatured the protein. Equal volumes containing 30.0 - 50.0 µg of total protein were loaded onto 4.0 - 20.0 % gradient gels (BioRad #456-8093). The proteins were then transferred to 0.2 µm Polyvinylidene Difluoride (PVDF) membranes (BioRad #170-4156) using the standard protocol for semi dry 30.0-minute Trans-blot Turbo transfer at 25.0 volts (V) and 1.0 ampere (AMP). Following transfer, the membrane was incubated in 2.5% glutaraldehyde (Sigma #G7651-10) allowing the cross linking of the proteins to the membrane for 60.0 minutes. The membranes where then blocked in 3.0% Bovine Serum Albumin (BSA) (Fisher Scientific #BP1605-100) dissolved in 10.0 mM Tris-Buffered Saline (TBS) (BioRad #170-6435) on the orbital shaker at room temperature for 120.0 minutes. The

membranes where then washed in 10.0 mM TBS and 1.0% Tween-20 (TBS-T) (Sigma

#P1379-500) before the overnight (16.0 hours) incubation of the primary antibody. After

the membranes were washed in TBS-T there were incubated for 90.0 minutes in the

secondary antibody on the orbital shaker at room temperature. Blots were visualized

using Clarity Western ECL Substrate (BioRad #170-5061).

Table II-6. Primary Antibodies used for Metallothionein Western Blot Analysis.						
Antibody	Dilution	Source & Clonality	Storage	Company	Catalog #	Mw (kDa)
MT, E9	1:200 (BSA)	Mouse Monoclonal	-20˚C	DAKO (Agilent)	M0639	6
β-Actin	1:5000 (BSA)	Mouse Monoclonal	-20˚C	Abcam	Ab8226	42

CHAPTER III.

Experimental Results.

Arsenite and Cadmium *In-vitro* Model System.

In order to study the mechanisms involved in early bladder cancer our laboratory strategically exposed the non-tumorigenic urothelial cell line UROtsa to long term treatment with As^{3+} or Cd^{2+} with the endpoint goal to determine if these heavy metals were capable of causing malignant cell transformation. The metal treated cells demonstrated a loss of the ability to stratify at confluency when compared to the Parent UROtsa, as well as, higher growth rates were also seen in the 1.0 µm As^{3+} or Cd^{2+} treated cells.

In order to further evaluate if these cells were able to cause malignant transformation they were plated on soft agar before being injected into nude mice. When plated the transformed cells showed colony formation, an indicator of anchorage independent growth. Additionally, the cells formed tumors when injected into nude mice. The histology of the tumors produced features consistent with those of classic TCC of bladder cancer. The heterotransplant tumors displayed prominent squamous differentiation. Therefore the

malignantly transformed UROtsa cell lines are an ideal model for studying bladder cancer. More details and all cell culture methods as described in the Methods and Materials. Cell culture media, buffers, and solution recipes are in Appendix B.

Real Time Reverse Transcriptase Quantitative Polymerase Chain Reaction.

Real time RT-qPCR analysis was performed on most of the MT isoforms (MT-1A, MT-1B, MT-1E, MT-1F, MT-1G, MT-1H, MT-1J, MT-1L, MT-1M, MT-1X, MT-2A, MT-3, and MT-4) however not all were continually used throughout the project. The MT isoforms that were focused on in this project are listed below in Table III-1, along with each isoforms corresponding size in base pairs.

All data was derived in an absolute fashion. Each standard curve was derived from serial dilution of the known purified PCR product at 10^8 transcripts stock of the target gene. The real time RT-qPCR was also normalized to Beta-Actin (β-Actin), which is a gene that is highly expressed in all cell types and is a known house-keeping gene. We know that a threshold cycle (C_t) value for β-Actin is roughly equal to 2.0×10^6 transcripts. The C_t is defined as the cycle number at which fluorescence generated within a reaction exceeds that of the background and is inversely proportional to the expression. For clarification the lower the C_t value the higher the gene expression. More details on real time RT-qPCR as described in the Methods and Materials. A brief introduction to real time RT-qPCR and extended explanation of C_t are found in Appendix C.

Table III-1. Metallothionein Isoforms evaluated in this Project.

The table below shows the MT isoforms that were used throughout this project. The table

also shows the base pairs that correspond with each isoform.

Table III-1. Metallothionein Isoforms evaluated in this Project.	
MT Isoforms	**Base Pairs**
MT-1A	219
MT-1E	284
MT-1F	232
MT-1X	151
MT-2A	259
MT-3	325

Basal Expression of Metallothioneins in the UROtsa Cell Lines.

The Parental UROtsa, six independent As^{3+} -transformed cell lines and seven independent Cd^{2+} -transformed cell lines, were assessed for their basal expression levels of the six MT isoforms (MT-1A, MT-1E, MT-1F, MT-1X, MT-2A, and MT-3). MT isoform 1A showed the Parent UROtsa cells displayed at a higher expression when compared to the minimal expression of the six independent As^{3+} cell lines and seven independent Cd^{2+} cell lines of the transformed cells (Figures III-1 and III-2, respectively). All 13 cell lines exhibited similar statistically significant expression compared to the Parent UROtsa.

For MT isoform 1E the expression was higher in the Parent UROtsa cells when compared to the As^{+3}-transformed cell lines (Figure III-3). This increase was statistically significant. The expression pattern was similar for the Cd^{+2}-transformed cell lines with the exception of Cd #7, which had increased expression when compared to the Parent UROtsa cells (Figure III-4).

The expression of MT isoform 1F was decreased in the As^{+3}-transformed cells when compared to the Parental UROtsa cells with one exception. The exception was As #4, which showed increased expression when compared to the Parental UROtsa cells. All expression changes were statistically significant (Figure III-5). For the Cd^{+2}-transformed cell lines, the expression of MT isoform 1F was decreased in three of the cell lines Cd #1, Cd #5, and Cd #6. Whereas the expression was increased compared to the Parent UROtsa cell line for Cd #7 (Figure III-6). There was no change in expression of MT isoform 1F in Cd #2, Cd #3, and Cd #4.

The expression of MT isoform 1X was similar between the Parent UROtsa and the As^{+3}-transformed cell lines with the exception of As #4, which had a higher expression compared to the Parent UROtsa. This increase in expression was statistically significant (Figure III-7). The expression of MT isoform 1X in the Cd^{+2}-transformed cell lines was similar in five of the seven transformed cell lines. For Cd #1 and Cd #7, the expression of MT isoform 1X was higher compared to the Parent UROtsa cells. This increase was also statistically significant (Figure III-8). Albeit the expression of MT isoform 1X was lower in the Cd #5 when compared to the Parent UROtsa, this decrease was not statistically significant.

The expression of MT isoform 2A was decreased in the all of the As^{+3}-transformed cell lines when compared to the Parent UROtsa cells. The decreased expression in all of the As^{+3}-transformed cell lines was statistically significant (Figure III-9). The Cd^{2+}-transformed cells showed decrease in expression of MT isoform 2A when compared to the Parent UROtsa in all of the cell lines with one exception. The exception being Cd #7, which showed an increase in expression compared to the Parental UROtsa cells. These expression levels were all statistically significant excluding Cd #7 (Figure III-10).

The expression of MT isoform 3 was very low in the Parent UROtsa, as well as, the transformed cell lines. There was a slight increase in As #1, As #2, As #3, As #4, and As #6, which were all statistically significant (Figure III-11). For the Cd^{+2}-transformed cells, the expression of MT isoform 3 was increased in Cd #1, Cd #3, Cd #5, and Cd #7 compared to the Parent UROtsa cells, while Cd #2, Cd #4, and Cd #6 showed similar expression to the Parent UROtsa (Figure III-12).
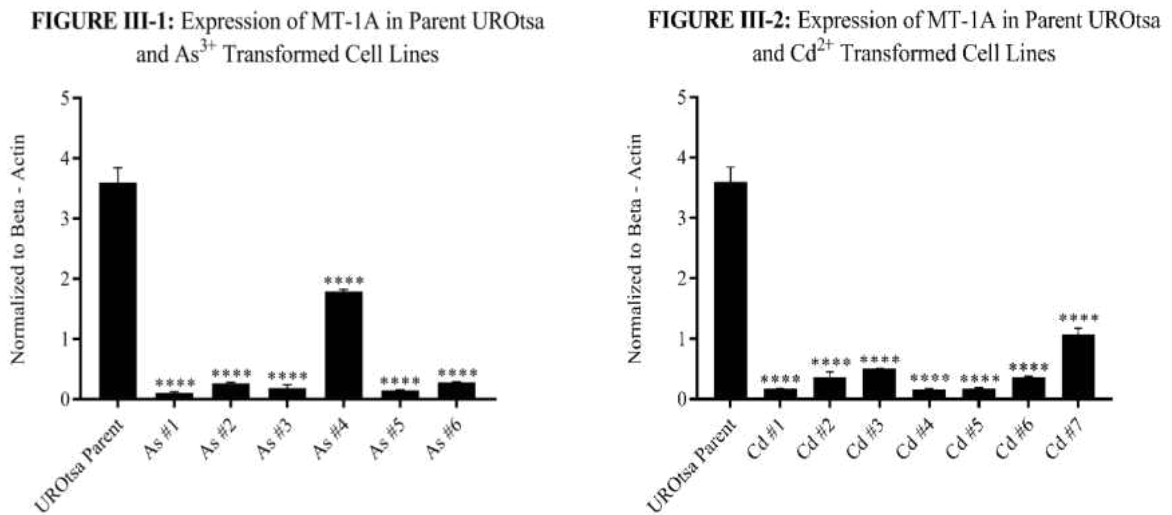
In summary, the expression of the MT isoforms in the As^{3+}-and Cd^{2+}-transformed cell lines is lower than that of the Parent UROtsa with a few exceptions. However, the expression of MT isoform 3 is very low in the Parent UROtsa as well as the As^{3+}-and Cd^{2+}-transformed cell lines as seen previously in literature.

Figure III-1. Expression of MT-1A in Parent UROtsa and As^{3+} Transformed Cell Lines. Real time RT-qPCR analysis of MT isoform 1A mRNA levels. The mRNA levels were normalized to β-Actin and are shown as relative mRNA levels ± SEM (n = 3) for the Parent UROtsa and the As^{3+} -transformed cell lines.

Figure III-2. Expression of MT-1A in Parent UROtsa and Cd^{2+} Transformed Cell Lines. Real time RT-qPCR analysis of MT isoform 1A mRNA levels. The mRNA levels were normalized to β-Actin and are shown as relative mRNA levels ± SEM (n = 3) for the Parent UROtsa and the Cd^{2+} -transformed cell lines.

FIGURE III-1: Expression of MT-1A in Parent UROtsa and As^{3+} Transformed Cell Lines
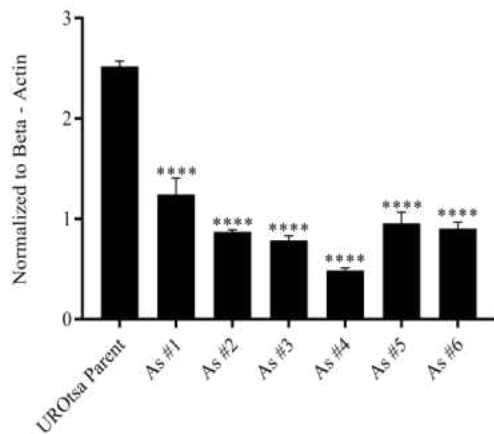
FIGURE III-2: Expression of MT-1A in Parent UROtsa and Cd^{2+} Transformed Cell Lines

For statistically significant changes in comparison to the Parent UROtsa.

* indicates $p<0.05$, ** indicates $p<0.01$, *** indicates $p<0.001$, and **** indicates $p<0.001$

Figure III-3. Expression of MT-1E in Parent UROtsa and As^{3+} Transformed Cell Lines. Real time RT-qPCR analysis of MT isoform 1E mRNA levels. The mRNA levels were normalized to β-Actin and are shown as relative mRNA levels ± SEM (n = 3) for the Parent UROtsa and the As^{3+} -transformed cell lines.

Figure III-4. Expression of MT-1E in Parent UROtsa and Cd^{2+} Transformed Cell Lines. Real time RT-qPCR analysis of MT isoform 1E mRNA levels. The mRNA levels were normalized to β-Actin and are shown as relative mRNA levels ± SEM (n = 3) for the Parent UROtsa and the Cd^{2+} -transformed cell lines.

FIGURE III-3: Expression of MT-1E in Parent UROtsa and As^{3+} Transformed Cell Lines
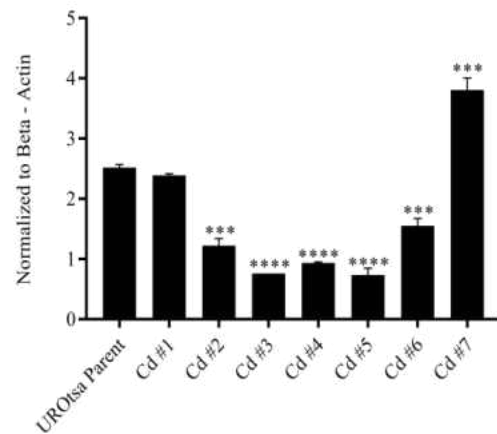
FIGURE III-4: Expression of MT-1E in Parent UROtsa and Cd^{2+} Transformed Cell Lines

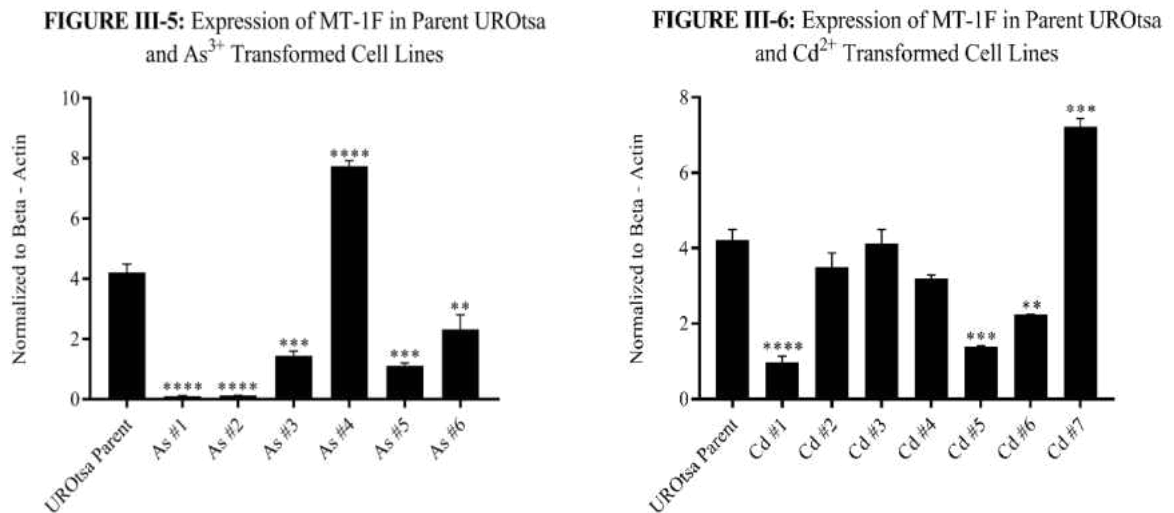For statistically significant changes in comparison to the Parent UROtsa.

 * indicates p<0.05, ** indicates p<0.01, *** indicates p<0.001, and **** indicates p<0.001

Figure III-5. Expression of MT-1F in Parent UROtsa and As^{3+} Transformed Cell

Lines. Real time RT-qPCR analysis of MT isoform 1F mRNA levels. The mRNA levels were normalized to β-Actin and are shown as relative mRNA levels ± SEM (n = 3) for the Parent UROtsa and the As^{3+} -transformed cell lines.

Figure III-6. Expression of MT-1F in Parent UROtsa and Cd^{2+} Transformed Cell

Lines. Real time RT-qPCR analysis of MT isoform 1F mRNA levels. The mRNA levels were normalized to β-Actin and are shown as relative mRNA levels ± SEM (n = 3) for the Parent UROtsa and the Cd^{2+} -transformed cell lines.

FIGURE III-5: Expression of MT-1F in Parent UROtsa and As^{3+} Transformed Cell Lines

FIGURE III-6: Expression of MT-1F in Parent UROtsa and Cd^{2+} Transformed Cell Lines

For statistically significant changes in comparison to the Parent UROtsa.
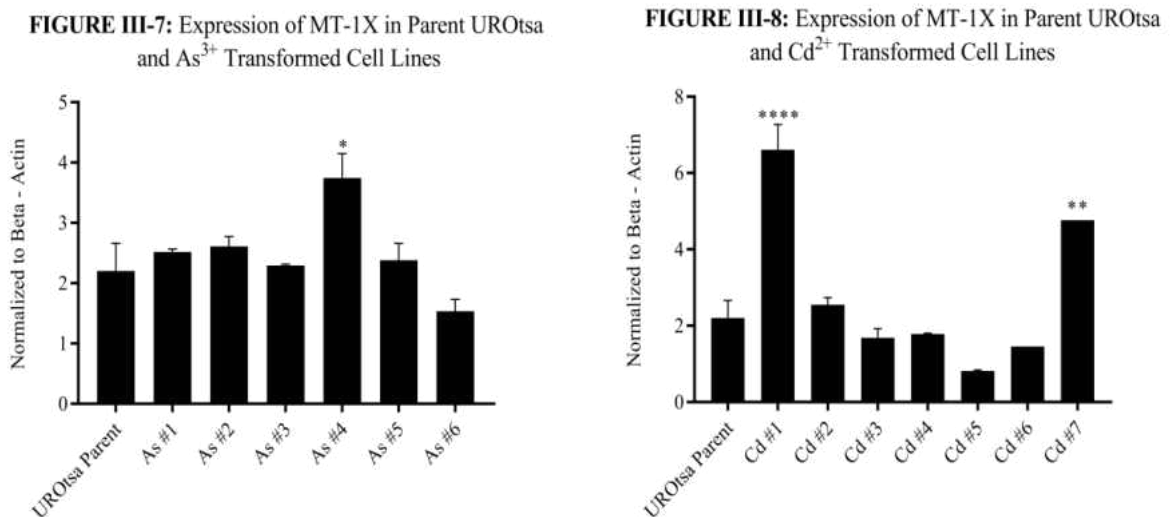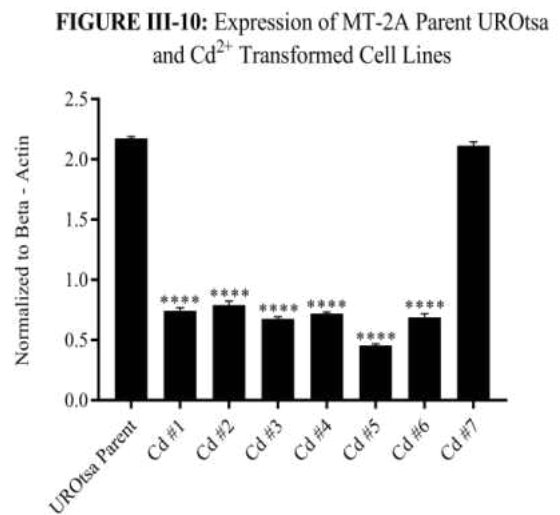
 * indicates $p<0.05$, ** indicates $p<0.01$, *** indicates $p<0.001$, and **** indicates $p<0.001$

Figure III-7. Expression of MT-1X in Parent UROtsa and As^{3+} Transformed Cell Lines. Real time RT-qPCR analysis of MT isoform 1X mRNA levels. The mRNA levels were normalized to β-Actin and are shown as relative mRNA levels ± SEM (n = 3) for the Parent UROtsa and the As^{3+} -transformed cell lines.

Figure III-8. Expression of MT-1X in Parent UROtsa and Cd^{2+} Transformed Cell Lines. Real time RT-qPCR analysis of MT isoform 1X mRNA levels. The mRNA levels were normalized to β-Actin and are shown as relative mRNA levels ± SEM (n = 3) for the Parent UROtsa and the Cd^{2+} -transformed cell lines.

FIGURE III-7: Expression of MT-1X in Parent UROtsa and As^{3+} Transformed Cell Lines

FIGURE III-8: Expression of MT-1X in Parent UROtsa and Cd^{2+} Transformed Cell Lines

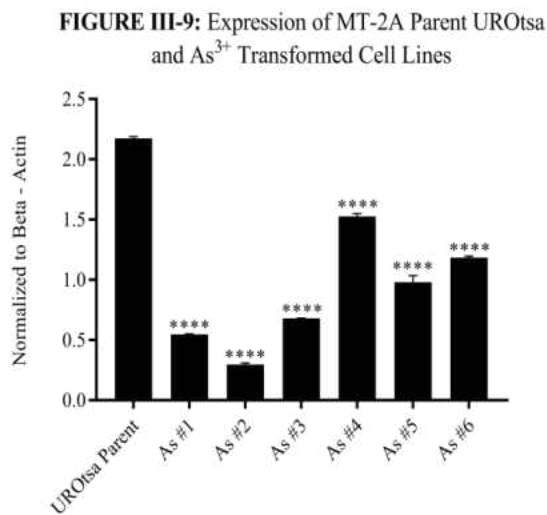For statistically significant changes in comparison to the Parent UROtsa.

 * indicates $p<0.05$, ** indicates $p<0.01$, *** indicates $p<0.001$, and **** indicates $p<0.001$

31

Figure III-9. Expression of MT-2A in Parent UROtsa and As^{3+} Transformed Cell Lines. Real time RT-qPCR analysis of MT isoform 2A mRNA levels. The mRNA levels were normalized to β-Actin and are shown as relative mRNA levels ± SEM (n = 3) for the Parent UROtsa and the As^{3+} -transformed cell lines.

Figure III-10. Expression of MT-2A in Parent UROtsa and Cd^{2+} Transformed Cell Lines. Real time RT-qPCR analysis of MT isoform 2A mRNA levels. The mRNA levels were normalized to β-Actin and are shown as relative mRNA levels ± SEM (n = 3) for the Parent UROtsa and the Cd^{2+} -transformed cell lines.

FIGURE III-9: Expression of MT-2A Parent UROtsa and As^{3+} Transformed Cell Lines

FIGURE III-10: Expression of MT-2A Parent UROtsa and Cd^{2+} Transformed Cell Lines

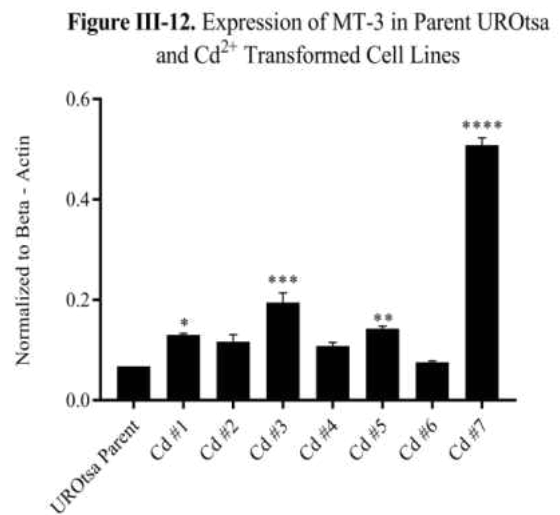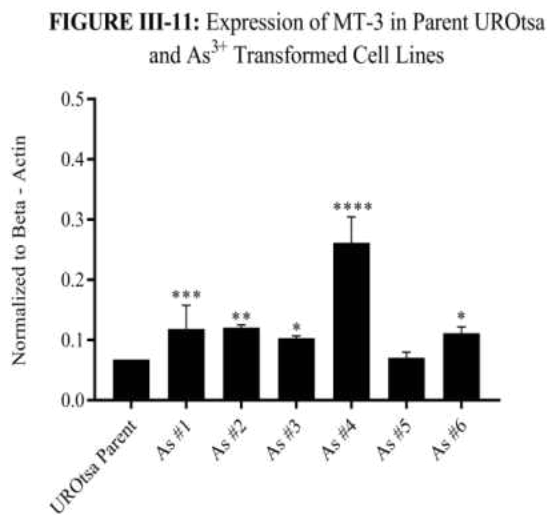For statistically significant changes in comparison to the Parent UROtsa.

 * indicates $p < 0.05$, ** indicates $p < 0.01$, *** indicates $p < 0.001$, and **** indicates $p < 0.001$

Figure III-11. Expression of MT-3 in Parent UROtsa and As³⁺ Transformed Cell Lines.
Real time RT-qPCR analysis of MT isoform 3 mRNA levels. The mRNA levels were normalized to β-Actin and are shown as relative mRNA levels ± SEM (n = 3) for the Parent UROtsa and the As³⁺ -transformed cell lines.

Figure III-12. Expression of MT-3 in Parent UROtsa and Cd²⁺ Transformed Cell Lines. Real time RT-qPCR analysis of MT isoform 3 mRNA levels. The mRNA levels were normalized to β-Actin and are shown as relative mRNA levels ± SEM (n = 3) for the Parent UROtsa and the Cd²⁺ -transformed cell lines.

FIGURE III-11: Expression of MT-3 in Parent UROtsa and As³⁺ Transformed Cell Lines

Figure III-12. Expression of MT-3 in Parent UROtsa and Cd²⁺ Transformed Cell Lines

For statistically significant changes in comparison to the Parent UROtsa.

 * indicates $p<0.05$, ** indicates $p<0.01$, *** indicates $p<0.001$, and **** indicates $p<0.001$

Immunohistochemistry Analysis Expression of Metallothioneins 1/2 and 3.

IHC staining was used to determine the localization of MT isoforms 1/2 and MT isoform 3 in the cells of the mouse heterotransplant tumors. IHC was performed in the histology core facility within the Department of Pathology by Dr. Xu Dong Zhou and the department technicians. Tissue sections for IHC analysis were prepared and visualized as described in the Methods and Materials.

MT isoforms 1/2 is an antibody that encompasses all the MT isoform 1 and MT isoform 2 since the genetic sequences are too similar to have two separate antibodies. MT isoforms 1/2 staining of the six As^{3+} and the seven Cd^{2+} UROtsa Subcutaneous Tumors show moderate or weak-to-moderate staining in all of the isolates. Only one tumor stained weakly positive for MT isoforms 1/2. The percentage of the positive staining ranges from 5.0% to 25.0%. Usually, it is the less differentiated basal-like cells in the invading border or periphery of tumor nests that are positive for MT isoforms 1/2. One tumor also shows strong positive MT isoforms 1/2 staining in the spindle tumor stroma cells (Figures III-13 and III-14).

All of the 13 UROtsa mouse subcutaneous tumors show strong and diffuse staining of MT isoform 3. However, in some tumors, the peripheral less differentiated tumor cells show weaker staining. Some tumor stroma cells are also positive for MT isoform 3, but the keratin pearls are negative. The percentage of the positive staining ranges from 60.0% to more than 80.0% (Figures III-15 and III-16).

Figure III-13, A - F. Immunohistochemistry of MT-1/2 in the As^{3+} Subcutaneous Tumors.

Immunohistochemical staining of MT isoforms 1/2 in the Mouse Subcutaneous Tumors from the six As^{3+} UROtsa Transformed Cell lines. **(A)** As #1 shows moderate positive staining of MT isoforms 1/2 in the less differentiated peripheral cells of tumor nests. **(B)** As #2 shows less differentiated tumor cells in the invading buds and the outside basal-like cells of tumor nests are moderately positive for MT isoforms 1/2. **(C)** As #3 shows less differentiated basal-like tumor cells that are weak-to-moderately positive for MT isoforms 1/2. The cells with vacuole cytoplasm in the center of tumor nests are negative for MT isoforms 1/2. **(D)** As #4 shows less differentiated tumor cells in the invading buds and peripheral basal-like cells are moderately positive for MT isoforms 1/2. The relatively well differentiated cells in the center of tumor nests are negative for MT isoforms 1/2. Two keratin pearls are also negative for MT isoforms 1/2. In addition to the moderate staining of MT isoforms 1/2 in the less differentiated tumor cells, the spindle tumor stroma cells are strongly positive for MT isoforms 1/2. **(E)** As #5 shows weak-to-moderate staining of MT isoforms 1/2 in the less differentiated tumor cells. **(F)** As # 6 shows weak-to-moderate staining of MT isoforms 1/2 in the less differentiated tumor cells.

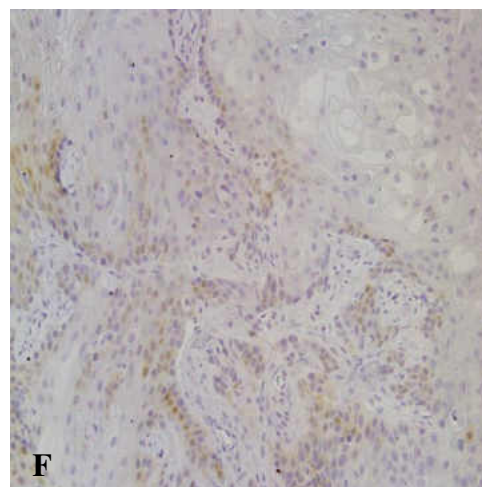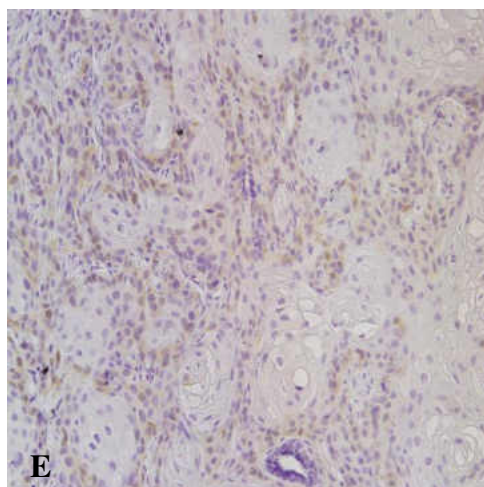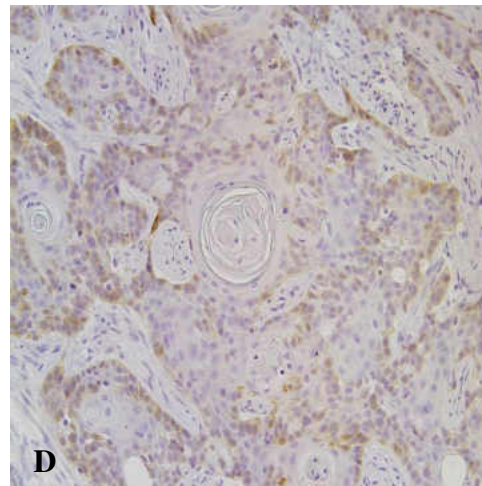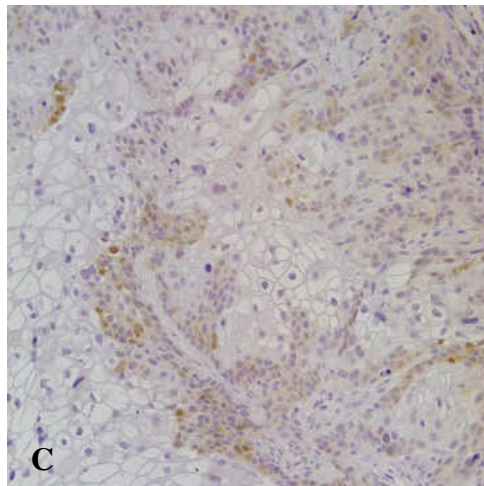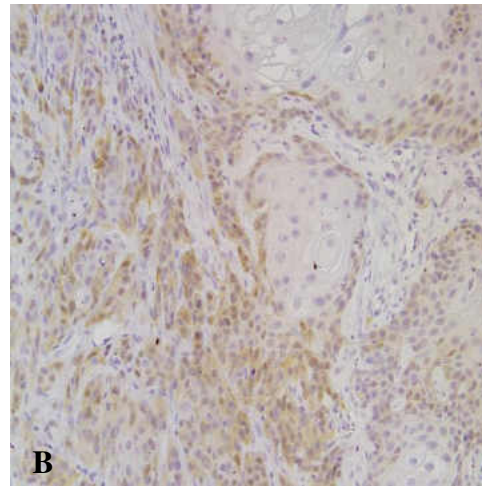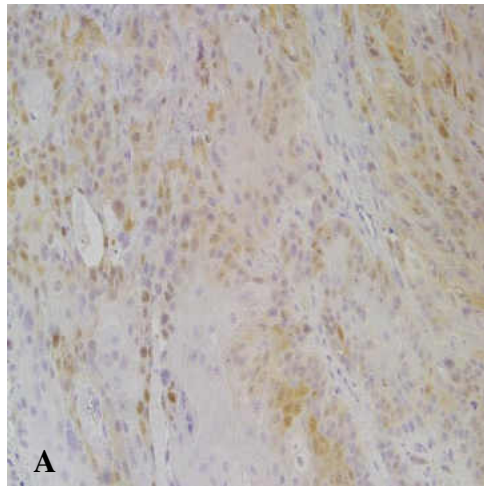All images taken at the magnification of X200.

Figure III-14, A - G. Immunohistochemistry of MT-1/2 in the Cd^{2+} Subcutaneous Tumors.

Immunohistochemical staining of MT isoforms 1/2 in the Mouse Subcutaneous Tumors from the seven Cd^{2+} UROtsa Transformed Cell lines. **(A)** Cd #1 shows a moderate staining of MT isoforms 1/2 in the less differentiated tumor cells. **(B)** Cd #2 shows a weak staining of MT isoforms 1/2 in the peripheral less differentiated tumor cells. **(C)** Cd #3 shows a weak-to-moderate staining of MT isoforms 1/2 in the peripheral less differentiated tumor cells. **(D)** Cd #4 shows a weak-to-moderate staining of MT isoforms 1/2 in the peripheral less differentiated tumor cells. **(E)** Cd #5 shows a moderate staining of MT isoforms 1/2 in invading buds and peripheral less differentiated tumor cells. **(F)** Cd #6 shows a weak-to-moderate staining of MT isoforms 1/2 in the peripheral less differentiated tumor cells. **(G)** Cd #7 shows a weak-to-moderate staining of MT isoforms 1/2 in the peripheral less differentiated tumor cells.
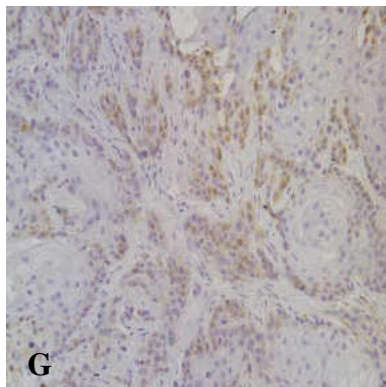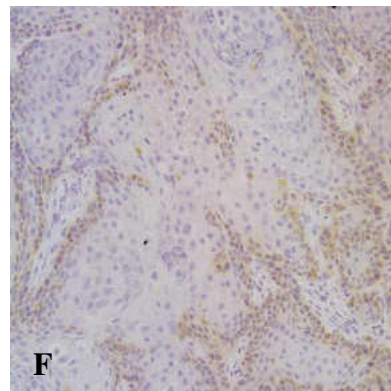
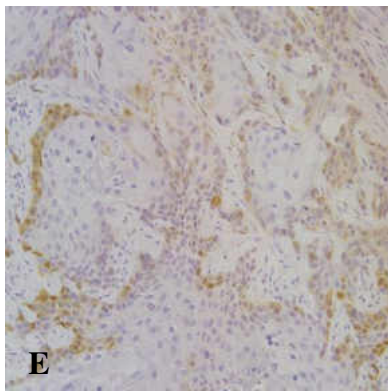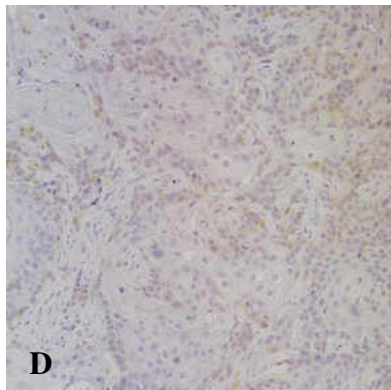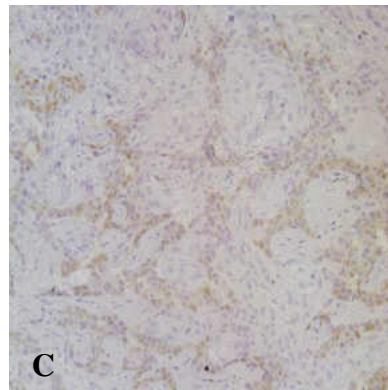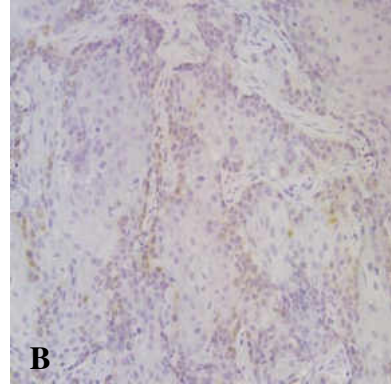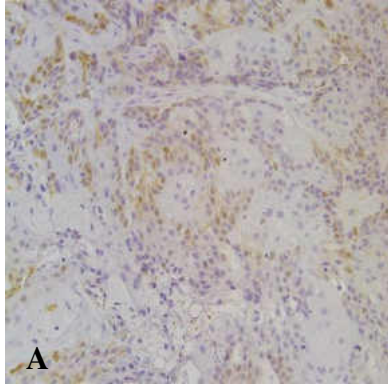All images taken at the magnification of X200.

Figure III-15, A - F. Immunohistochemistry of MT-3 in the As^{3+} Subcutaneous Tumors.

Immunohistochemical staining of MT isoform 3 in the Mouse Subcutaneous Tumors from the six As^{3+} UROtsa Transformed Cell lines. **(A)** As #1 demonstrated diffused and strong positive staining for MT isoform 3. Some less differentiated peripheral cells show weaker staining of MT isoform 3, while the Keratin pearls are negative for MT isoform 3. **(B)** As #2 demonstrated diffused and strong positive staining for MT isoform 3. The tumor stroma cells are also positive for MT isoform 3. **(C)** As #3 demonstrated diffused and strong positive staining for MT isoform 3, but the large cells with vacuole cytoplasm in the center of tumor nests show much weaker staining of MT isoform 3. **(D)** As #4 demonstrated diffused and strong positive staining for MT isoform 3. The tumor stroma cells are also positive for MT isoform 3. The keratin pearls are almost all negative for MT isoform 3. **(E)** As #5 demonstrated diffused and strong positive staining for MT isoform 3. The tumor stroma cells are also positive for MT isoform 3. The large cells with vacuole cytoplasm in the center of tumor nests show much weaker staining of MT isoform 3**. (F)** As #6 demonstrated diffused and strong positive staining for MT isoform 3. The tumor stroma cells are also positive for MT isoform 3. The less differentiated tumor cells show weaker staining of MT isoform 3. The keratin material in the center of tumor nests shows much weaker or no staining of MT isoform 3.

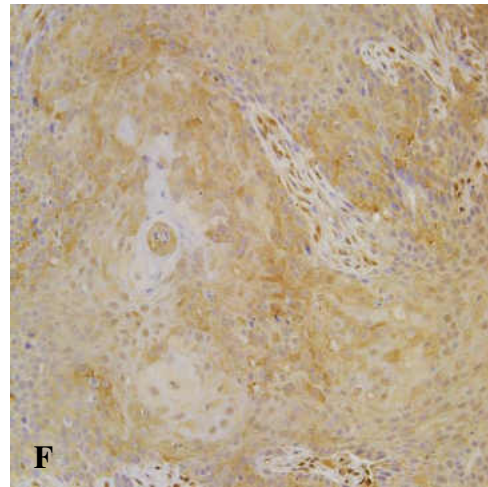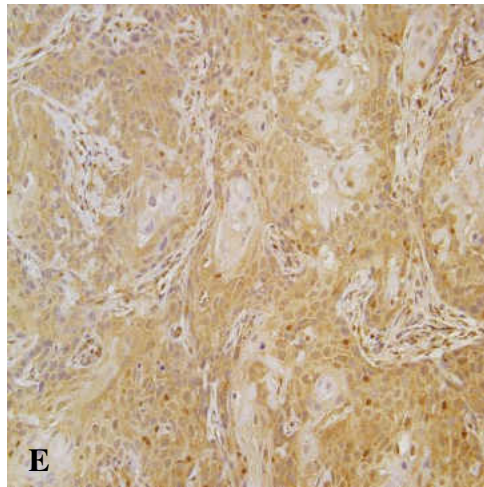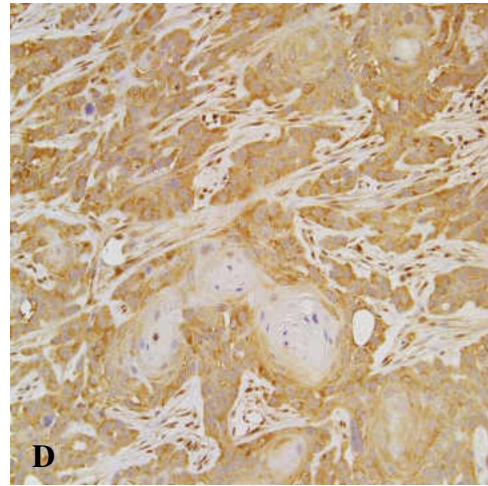All images taken at the magnification of X200.
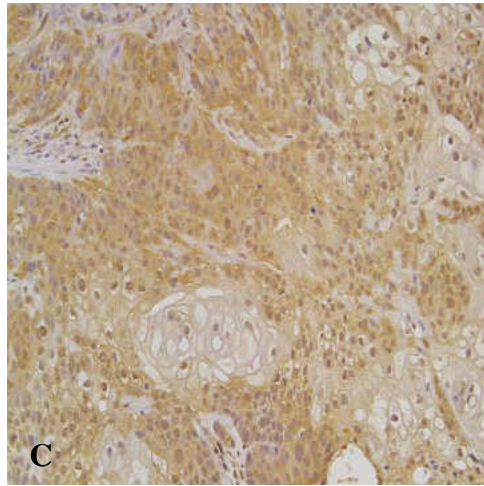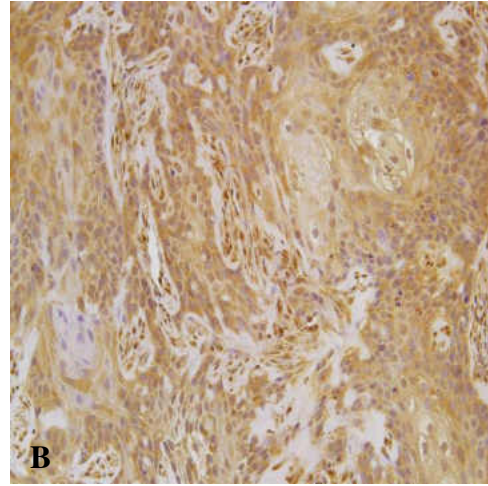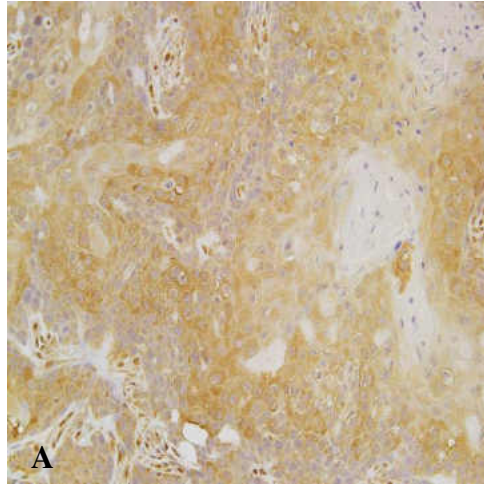
Figure III-16, A - G. Immunohistochemistry of MT-3 in the Cd^{2+} Subcutaneous Tumors.

Immunohistochemical staining of MT isoform 3 in the Mouse Subcutaneous Tumors from the seven Cd^{2+} UROtsa Transformed Cell lines. **(A)** Cd #1 demonstrated diffused and strong positive staining for MT isoform 3. The keratin material is almost all negative for MT isoform 3. **(B)** Cd #2 demonstrated diffused and strong positive staining for MT isoform 3. Some stroma cells are also positive for MT isoform 3. **(C)** Cd #3 demonstrated diffused and strong positive staining for MT isoform 3. The peripheral less differentiated tumor cells show weaker staining. **(D)** Cd #4 shows weak-to-moderate staining of MT isoform 3 in the peripheral less differentiated tumor cells. **(E)** Cd #5 demonstrated diffused and strong positive staining for MT isoform 3. **(F)** Cd #6 demonstrated diffused and strong positive staining for MT isoform 3. Some tumor stroma cells are also positive for MT isoform 3. The keratin pearls are negative for MT isoform 3. **(G)** Cd #7 demonstrated diffused and strong positive staining for MT isoform 3. The peripheral less differentiated tumor cells show a weaker staining of MT isoform 3.


All images taken at the magnification of X200.
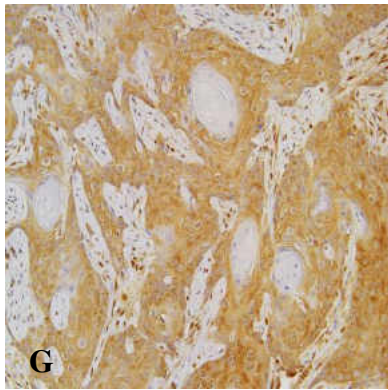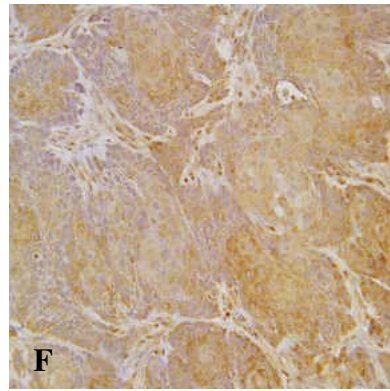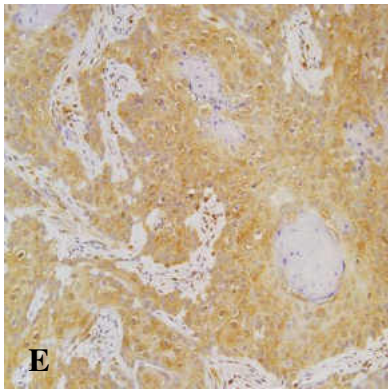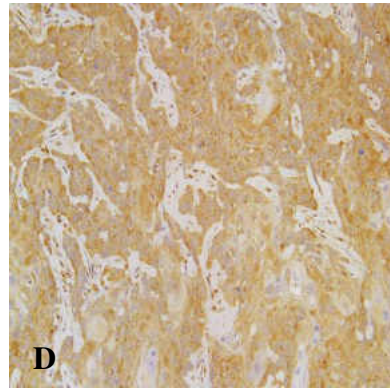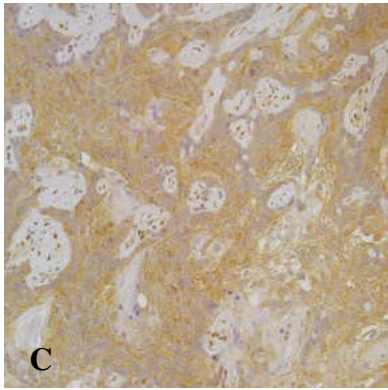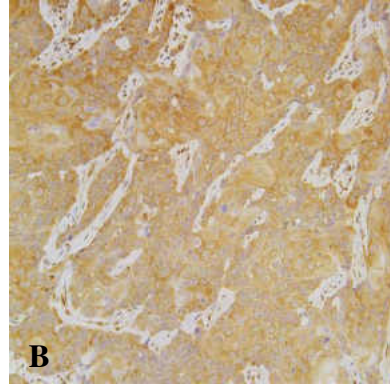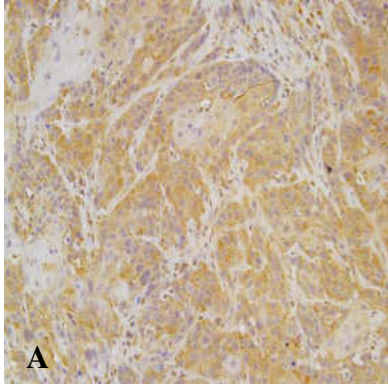
Exposure to Cisplatin Pilot Study.

In order to determine the growth effects of exposure to cisplatin on the Parent UROtsa and two As^{3+} (As #1 and As #5) -and two Cd^{2+} (Cd #1 and Cd #4) -transformed cell lines MTT assays were performed. In order to determine the growth rate, MTT assays were performed on cells dosed at 0.1 µg/mL, 0.25 µg/mL, 0.5 µg/mL, 1.0 µg/mL, and 2.0 µg/mL. The growth rates were tested on each day for three days. The data obtained shows as cisplatin increases that growth rates decrease in the UROtsa cell lines (Figure III-17, A-E). The higher doses also began to show signs of toxicity and cell death in the higher doses, especially on the third day. To effectively evaluate the effect of cisplatin on MT expression the cells need to be replicating in order to uptake the drug. Therefore, the doses that will be used throughout the rest of this study are 0.5 µg/mL and 1.0 µg/mL of cisplatin for two days.

Figure III-17, A-E. Effect of Cisplatin on the Growth Rate of the Parent UROtsa Cell Line.

The growth rates were determined by measuring the capacity of the cells to reduce MTT (3-(4, 5-dimethylthiazol2-yl)-2, 5-diphenyltetrazolium bromide) to formazan. The cells were allowed to grow for six days and the ability of the cells to reduce MTT was determined every day. All experiments were done in triplicates and shown is the mean absorbance value is shown. **(A)** Effect of Cisplatin on the Growth Rate of the Parent UROtsa Cell Line. **(B)** Effect of Cisplatin on the Growth Rate of the UROtsa As #1 -Transformed Cell Line. **(C)** Effect of Cisplatin on the Growth Rate of the UROtsa As #5 -Transformed Cell Line. **(D)** Effect of Cisplatin on the Growth Rate of the UROtsa Cd #1 -Transformed Cell Line. **(E)** Effect of Cisplatin on the Growth Rate of the UROtsa Cd #4 -Transformed Cell Line.

FIGURE III-17, A: Effect of Cisplatin on the Growth Rate of Parent UROtsa Cell Line
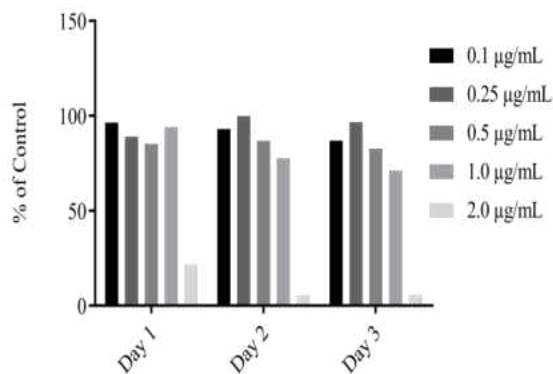

FIGURE III-17, B: Effect of Cisplatin on the Growth Rate of UROtsa As #1 Transformed Cell Line
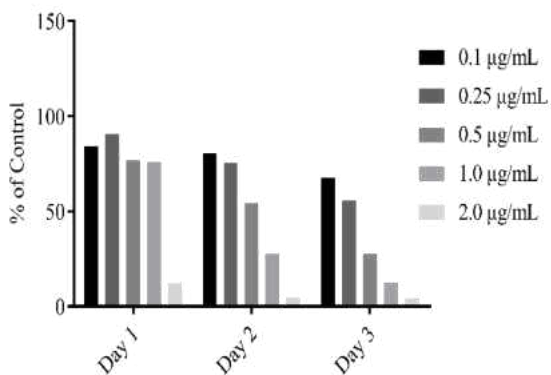
FIGURE III-17, C: Effect of Cisplatin on the Growth Rate of UROtsa As #5 Transformed Cell Line
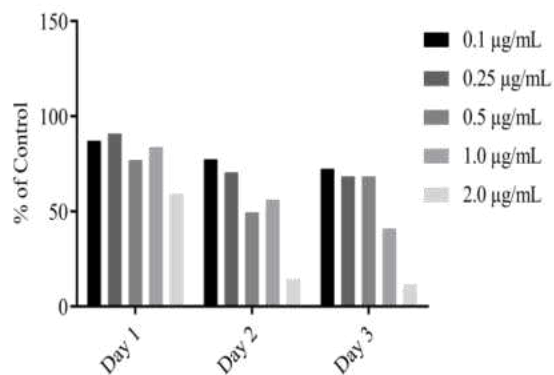
FIGURE III-17, D: Effect of Cisplatin on the Growth Rate of UROtsa Cd #1 Transformed Cell Line
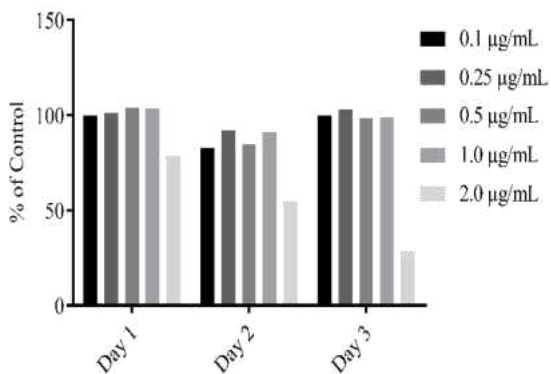
FIGURE III-17, E: Effect of Cisplatin on the Growth Rate of the UROtsa Cd #4 Transformed Cell Line
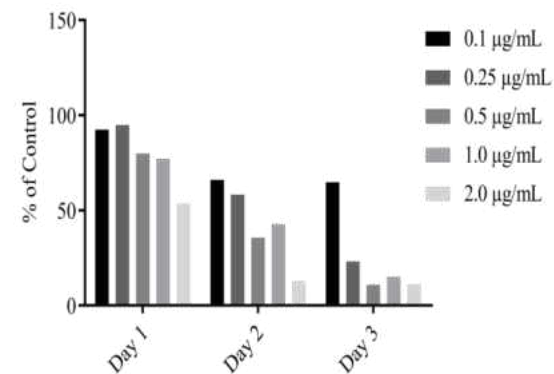
Expression of Metallothioneins exposed to Cisplatin in Real Time RT-qPCR.

The expression of MT isoforms was determined in Parent UROtsa cells and two As^{3+} (As #1 and As #5) -and two Cd^{2+} (Cd #1 and Cd #4) -transformed cell lines that were exposed to various doses of the chemotherapeutic drug cisplatin by real time RT-qPCR and Western Blot analysis. For this study As #1 and Cd #1 were picked because they can from intraperitoneal tumors, while As #5 and Cd #4 cannot form intraperitoneal tumors. This allows us to see if there is a difference in MT expression after exposure to cisplatin in all five cell lines. All five cell lines were dosed with 0.5 µg/mL and 1.0 µg/mL of cisplatin near confluency and the cells were harvested after Day #1 (24-hours) and Day #2 (48-hours). Real time RT-qPCR was performed on all six MT isoforms (MT-1A, MT-1E, MT-1F, MT-1X, MT-2A and MT-3) in the Parent UROtsa and the As^{3+}-and Cd^{2+}-transformed cell lines.

In the Parental cell line, there was no significant change in the expression levels of MT isoform 1A (Figure III-18, A). For the As^{3+}-transformed cell lines, there was a significant increase in the expression of MT isoform 1A in As #1, when the cells were treated with 1.0 µg/mL of cisplatin for Day #1 (24-hours) (Figure III-18, B). There was no significant change in expression levels of MT isoform 1A in As #5 (Figure III-18, C). For Cd #1, the expression of MT isoform 1A decreased after Day #2 (48-hours) treatment with cisplatin (Figure III-18, D), however no change in expression levels were noted for Cd #4 (Figure III-18, E).

The expression of MT isoform 1E was decreased in the Parental UROtsa cell line when treated with 1.0 µg/mL of cisplatin for Day #1 (24-hours). However, after Day #2 (48-

46

hours) there was no difference in expression between the control and the treated cells (Figure III-19, A). For the As^{3+}-and Cd^{2+} -transformed cell lines, for As #1, there was a decrease in expression of MT isofrom1E in cells exposed to cisplatin treated cells for Day #1 (24-hours) and this decrease was also seen after Day #2 (48-hours) exposure (Figure III-19, B). However, for As #5, there was no significant change in the level of expression of MT isoform 1E even after Day #2 (48-hours) of exposure (Figure III-19, C). For Cd#1 and Cd#4, exposure to cisplatin at both doses resulted in a decrease in the expression of MT isoform 1E and this decrease persisted throughout the Day #2 (48-hours) exposure (Figures III-19, D-E).

The expression of MT isoform1F showed a decrease after Day #1 (24-hours) exposure to cisplatin at 1.0 µg/mL and after Day #2 (48-hours) of exposure. There was also a decrease in expression at both 0.5 and 1.0 µg/mL of cisplatin (Figure III-20, A). For the As^{3+}-transformed cell lines, As #1 and As #5, there was decrease in expression of MT isoform 1F at both doses after Day #1 (24-hours) exposure and this decrease persisted up to Day #2 (48-hours) of treatment (Figures III-20, B-C). The expression of MT isoform 1F in the Cd^{2+}-transformed cell line Cd #1 was similar to the untreated controls, whereas for Cd #4, there was a decrease in expression at both doses up to Day #2 (48-hours) of treatment (Figures III-20, D-E).

The basal expression of MT isoform 1X was low in all the five cell lines. For the Parent UROtsa cells, treatment with cisplatin at doses of 0.5 µg/mL and 1.0 µg/mL resulted in a decrease in expression of MT isoform 1X at Day #2 (48-hours). There was no effect of cisplatin at either of the doses after Day #1 (24-hours) of exposure (Figure III-21, A). For the As^{3+}-transformed cell lines, there was a decrease in expression of MT isoform 1X after Day #2 (48-hours) of treatment with 1.0 µg/mL of cisplatin (Figures III-21, B-C). For Cd #1,

47

there was a decrease in expression after Day #1 (24-hours) and Day #2 (48-hours) of treatment with both 0.5 and 1.0 µg/mL of cisplatin. For Cd #4, there was not effect on the expression of MT isoform 1X after treatment with cisplatin (Figures III-21, D-E).

Exposure to cisplatin had no effect on the expression levels of MT isoform 2A in the Parent UROtsa cells (Figure III-22, A). For the As^{3+}-transformed cell lines, there was a decrease in expression of MT isoform 2A in As #1, whereas exposure to cisplatin had no effect on the expression levels of MT isoform 2A in As #5 (Figures III-22, B-C). The expression of MT isoform 2A decreased in both Cd #1 and Cd #4 when the cells were exposed to cisplatin for Day #1 (24-hours) and Day #2 (48-hours) (Figures III-22, D-E).

The final MT isoform that was evaluated through real time RT-qPCR was MT isoform 3. The basal expression of MT isoform 3 in the Parent UROtsa and the transformed cell lines is very low and treatment with cisplatin had no effect on the expression levels of MT isoform 3 in the Parent UROtsa as well as the transformed cell lines (Figures III-23, A-E).

Figure III-18, A-E. Expression of MT-1A in UROtsa Cell Line exposed to Cisplatin.

Real-time RT-qPCR analysis of MT isoform 1A mRNA levels that were treated with 0.0 µg/mL, 0.5 µg/mL and 1.0 µg/mL of cisplatin over a two day treatment. The mRNA levels were normalized to β-Actin and are shown as relative mRNA levels ±SEM (n=3) for the Parent UROtsa and UROtsa cell lines transformed with As^{3+} or Cd^{2+}. **(A)** Expression of MT-1A in UROtsa Cell Line exposed to cisplatin. **(B)** Expression of MT-1A in As #1 Transformed Cell Line exposed to cisplatin. **(C)** Expression of MT-1A in As #5 Transformed Cell Line exposed to cisplatin. **(D)** Expression of MT-1A in Cd #1 Transformed Cell Line exposed to cisplatin. **(E)** Expression of MT-1A in Cd #4 Transformed Cell Line exposed to cisplatin.

For statistically significant changes in comparison to the Control (0.0 µg/mL) Day #1 or Control (0.0 µg/mL) Day #2, respectively.

* indicates $p<0.05$, ** indicates $p<0.01$, *** indicates $p<0.001$, and **** indicates $p<0.001$

FIGURE III-18, A: Expression of MT-1A in UROtsa Parent
Cell Line exposed to Cisplatin

FIGURE III-18, B: Expression of MT-1A in As #1 Transformed
Cell Line exposed to Cisplatin

FIGURE III-18, C: Expression of MT-1A in As #5 Transformed
Cell Line exposed to Cisplatin

FIGURE III-18, D: Expression of MT-1A in Cd #1 Transformed
Cell Line exposed to Cisplatin

FIGURE III-18, E: Expression of MT-1A in Cd #4 Transformed
Cell Line exposed to Cisplatin

Figure III-19, A-E. Expression of MT-1E in UROtsa Cell Line exposed to Cisplatin.

Real-time RT-qPCR analysis of MT isoform 1E mRNA levels that were treated with 0.0 µg/mL, 0.5 µg/mL and 1.0 µg/mL of cisplatin over a two day treatment. The mRNA levels were normalized to β-Actin and are shown as relative mRNA levels ±SEM (n=3) for the Parent UROtsa and UROtsa cell lines transformed with As^{3+} or Cd^{2+}. **(A)** Expression of MT-1E in UROtsa Cell Line exposed to cisplatin. **(B)** Expression of MT-1E in As #1 Transformed Cell Line exposed to cisplatin. **(C)** Expression of MT-1E in As #5 Transformed Cell Line exposed to cisplatin. **(D)** Expression of MT-1E in Cd #1 Transformed Cell Line exposed to cisplatin. **(E)** Expression of MT-1E in Cd #4 Transformed Cell Line exposed to cisplatin.

For statistically significant changes in comparison to the Control (0.0 µg/mL) Day #1 or Control (0.0 µg/mL) Day #2, respectively.

* indicates $p < 0.05$, ** indicates $p < 0.01$, *** indicates $p < 0.001$, and **** indicates $p < 0.001$

FIGURE III-19, A: Expression of MT-1E in UROtsa Parent Cell Line exposed to Cisplatin
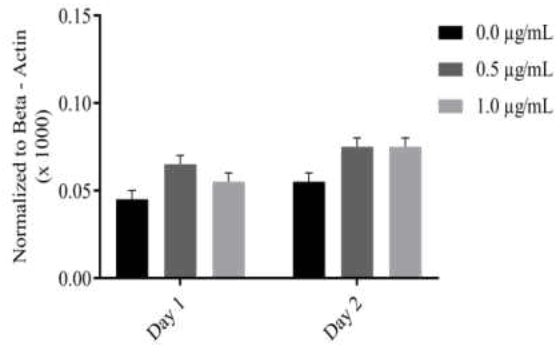
FIGURE III-19, B: Expression of MT-1E in As #1 Transformed Cell Line exposed to Cisplatin

FIGURE III-19, C: Expression of MT-1E in As #5 Transformed Cell Line exposed to Cisplatin

FIGURE III-19, D: Expression of MT-1E in Cd #1 Transformed Cell Line exposed to Cisplatin

FIGURE III-19, E: Expression of MT-1E in Cd #4 Transformed Cell Line exposed to Cisplatin

Figure III-20, A-E. Expression of MT-1F in UROtsa Cell Line exposed to Cisplatin.

Real-time RT-qPCR analysis of MT isoform 1F mRNA levels that were treated with 0.0 µg/mL, 0.5 µg/mL and 1.0 µg/mL of cisplatin over a two day treatment. The mRNA levels were normalized to β-Actin and are shown as relative mRNA levels ±SEM (n=3) for the Parent UROtsa and UROtsa cell lines transformed with As^{3+} or Cd^{2+}. **(A)** Expression of MT-1F in UROtsa Cell Line exposed to cisplatin. **(B)** Expression of MT-1F in As #1 Transformed Cell Line exposed to cisplatin. **(C)** Expression of MT-1F in As #5 Transformed Cell Line exposed to cisplatin. **(D)** Expression of MT-1F in Cd #1 Transformed Cell Line exposed to cisplatin. **(E)** Expression of MT-1F in Cd #4 Transformed Cell Line exposed to cisplatin.

For statistically significant changes in comparison to the Control (0.0 µg/mL) Day #1 or Control (0.0 µg/mL) Day #2, respectively.

* indicates $p < 0.05$, ** indicates $p < 0.01$, *** indicates $p < 0.001$, and **** indicates $p < 0.001$

FIGURE III-20, A: Expression of MT-1F in UROtsa Parent
Cell Line exposed to Cisplatin

FIGURE III-20, B: Expression of MT-1F in As #1 Transformed
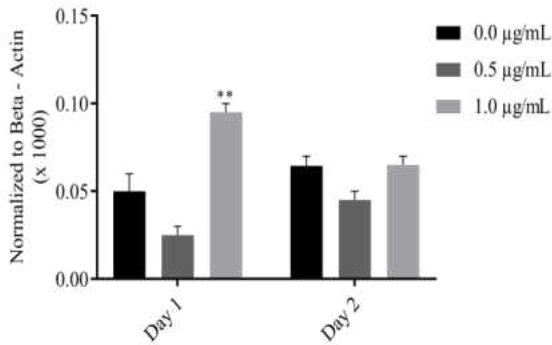Cell Line exposed to Cisplatin

FIGURE III-20, C: Expression of MT-1F in As #5 Transformed
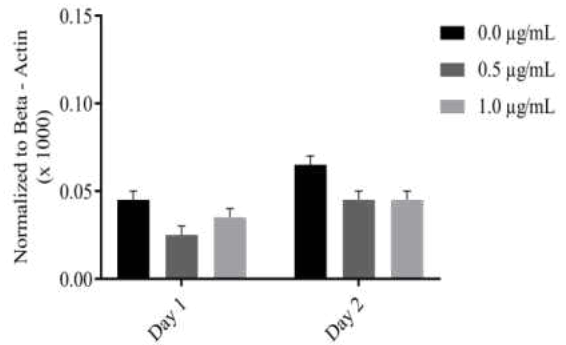Cell Line exposed to Cisplatin

FIGURE III-20, D: Expression of MT-1F in Cd #1 Transformed
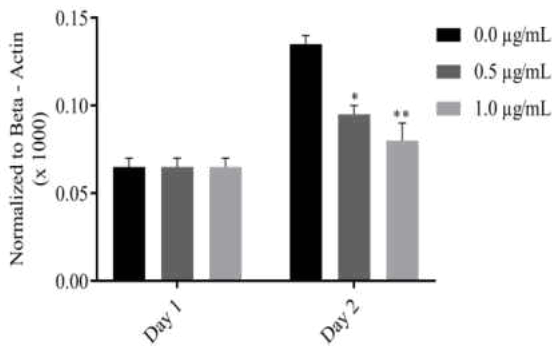Cell Line exposed to Cisplatin

FIGURE III-20, E: Expression of MT-1F in Cd #4 Transformed
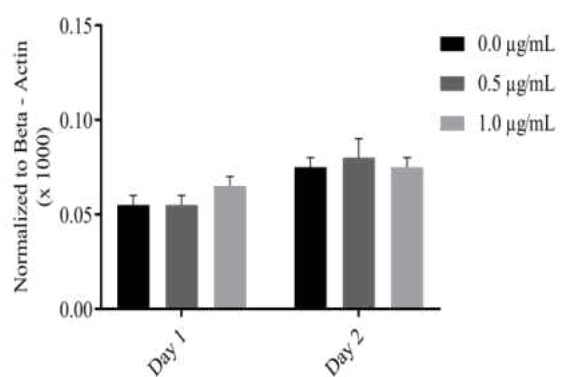Cell Line exposed to Cisplatin

54

Figure III-21, A-E. Expression of MT-1X in UROtsa Cell Line exposed to Cisplatin.

Real-time RT-qPCR analysis of MT isoform 1X mRNA levels that were treated with 0.0 µg/mL, 0.5 µg/mL and 1.0 µg/mL of cisplatin over a two day treatment. The mRNA levels were normalized to β-Actin and are shown as relative mRNA levels ±SEM (n=3) for the Parent UROtsa and UROtsa cell lines transformed with As^{3+} or Cd^{2+}. **(A)** Expression of MT-1X in UROtsa Cell Line exposed to cisplatin. **(B)** Expression of MT-1X in As #1 Transformed Cell Line exposed to cisplatin. **(C)** Expression of MT-1X in As #5 Transformed Cell Line exposed to cisplatin. **(D)** Expression of MT-1X in Cd #1 Transformed Cell Line exposed to cisplatin. **(E)** Expression of MT-1X in Cd #4 Transformed Cell Line exposed to cisplatin.

For statistically significant changes in comparison to the Control (0.0 µg/mL) Day #1 or Control (0.0 µg/mL) Day #2, respectively.

* indicates $p<0.05$, ** indicates $p<0.01$, *** indicates $p<0.001$, and **** indicates $p<0.001$

FIGURE III-21, A: Expression of MT-1X in UROtsa Parent
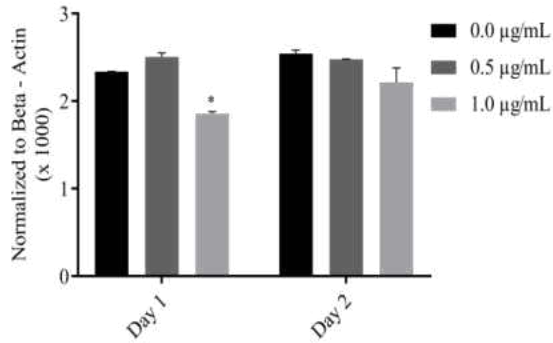Cell Line exposed to Cisplatin

FIGURE III-21, B: Expression of MT-1X in As #1 Transformed
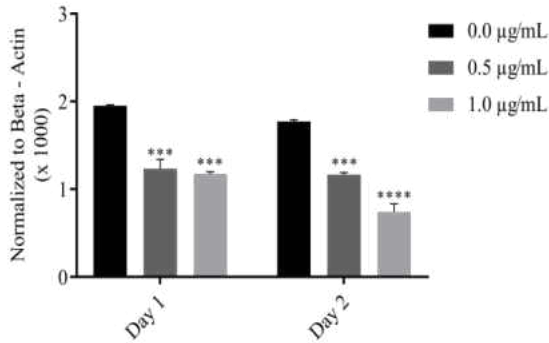Cell Line exposed to Cisplatin

FIGURE III-21, C: Expression of MT-1X in As #5 Transformed
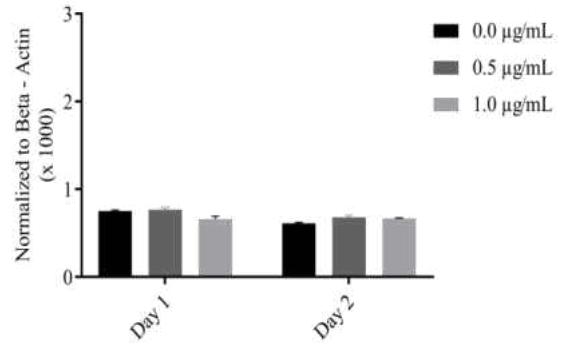Cell Line exposed to Cisplatin

FIGURE III-21, D: Expression of MT-1X in Cd #1 Transformed
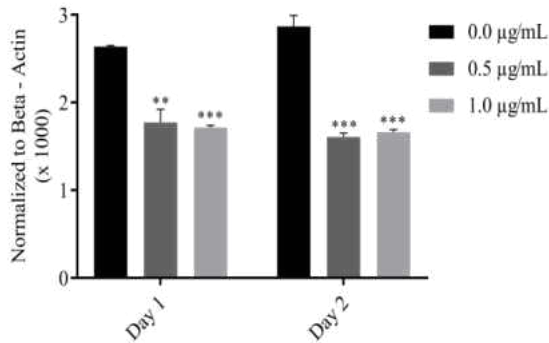Cell Line exposed to Cisplatin

FIGURE III-21, E: Expression of MT-1X in Cd #4 Transformed
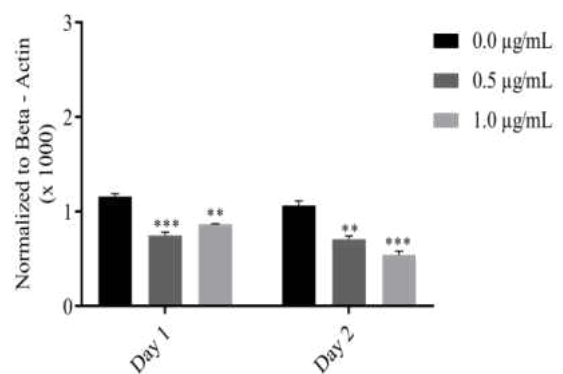Cell Line exposed to Cisplatin

56
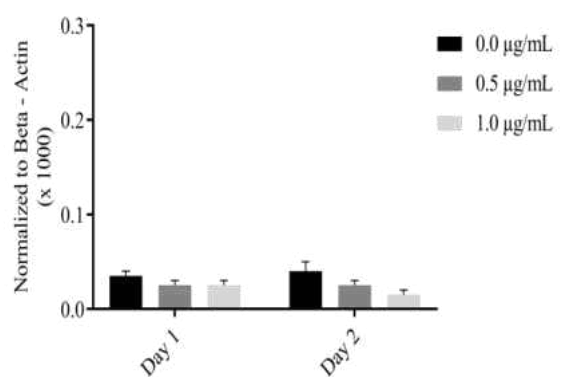
Figure III-22, A-E. Expression of MT-2A in UROtsa Cell Line exposed to Cisplatin.

Real-time RT-qPCR analysis of MT isoform 2A mRNA levels that were treated with 0.0 µg/mL, 0.5 µg/mL and 1.0 µg/mL of cisplatin over a two day treatment. The mRNA levels were normalized to β-Actin and are shown as relative mRNA levels ±SEM (n=3) for the Parent UROtsa and UROtsa cell lines transformed with As^{3+} or Cd^{2+}. **(A)** Expression of MT-2A in UROtsa Cell Line exposed to cisplatin. **(B)** Expression of MT-2A in As #1 Transformed Cell Line exposed to cisplatin. **(C)** Expression of MT-2A in As #5 Transformed Cell Line exposed to cisplatin. **(D)** Expression of MT-2A in Cd #1 Transformed Cell Line exposed to cisplatin. **(E)** Expression of MT-2A in Cd #4 Transformed Cell Line exposed to cisplatin.

For statistically significant changes in comparison to the Control (0.0 µg/mL) Day #1 or Control (0.0 µg/mL) Day #2, respectively.

* indicates $p < 0.05$, ** indicates $p < 0.01$, *** indicates $p < 0.001$, and **** indicates $p < 0.001$

FIGURE III-22, A: Expression of MT-2A in UROtsa Parent Cell Line exposed to Cisplatin
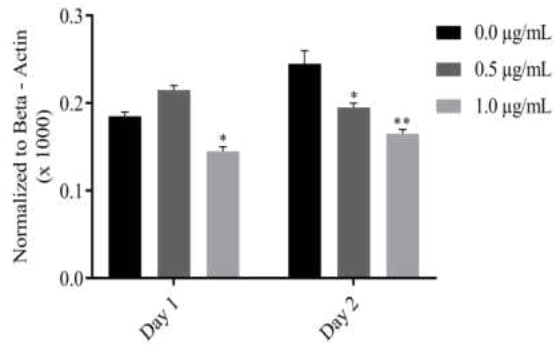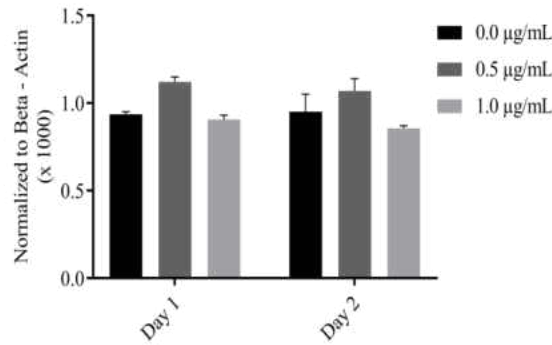

FIGURE III-22, B: Expression of MT-2A in As #1 Transformed Cell Line exposed to Cisplatin
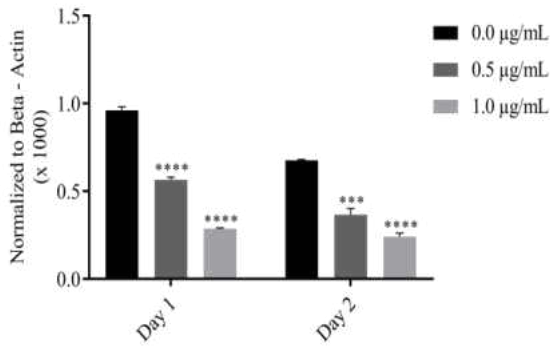
FIGURE III-22, C: Expression of MT-2A in As #5 Transformed Cell Line exposed to Cisplatin
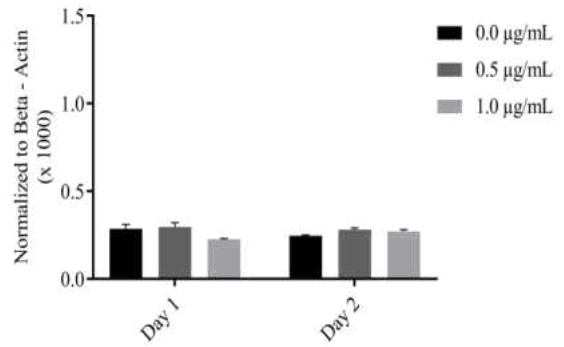
FIGURE III-22, D: Expression of MT-2A in Cd #1 Transformed Cell Line exposed to Cisplatin
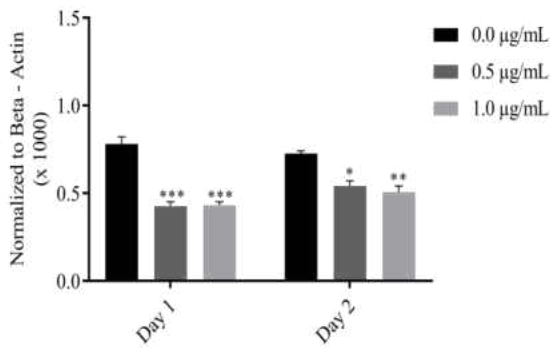
FIGURE III-22, E: Expression of MT-2A in Cd #4 Transformed Cell Line exposed to Cisplatin
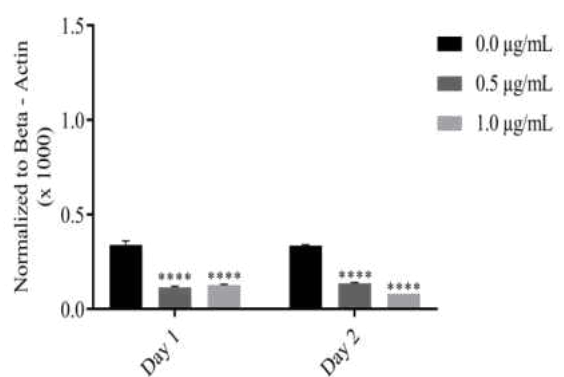
Figure III-23, A-E. Expression of MT-3 in UROtsa Cell Line exposed to Cisplatin.

Real-time RT-qPCR analysis of MT isoform 3 mRNA levels that were treated with 0.0 µg/mL, 0.5 µg/mL and 1.0 µg/mL of cisplatin over a two day treatment. The mRNA levels were normalized to β-Actin and are shown as relative mRNA levels ±SEM (n=3) for the Parent UROtsa and UROtsa cell lines transformed with As^{3+} or Cd^{2+}. **(A)** Expression of MT-3 in UROtsa Cell Line exposed to cisplatin. **(B)** Expression of MT-3 in As #1 Transformed Cell Line exposed to cisplatin. **(C)** Expression of MT-3 in As #5 Transformed Cell Line exposed to cisplatin. **(D)** Expression of MT-3 in Cd #1 Transformed Cell Line exposed to cisplatin. **(E)** Expression of MT-3 in Cd #4 Transformed Cell Line exposed to cisplatin.

For statistically significant changes in comparison to the Control (0.0 µg/mL) Day #1 or Control (0.0 µg/mL) Day #2, respectively.

* indicates $p < 0.05$, ** indicates $p < 0.01$, *** indicates $p < 0.001$, and **** indicates $p < 0.001$

FIGURE III-23, A: Expression of MT-3 in UROtsa Parent Cell Line exposed to Cisplatin
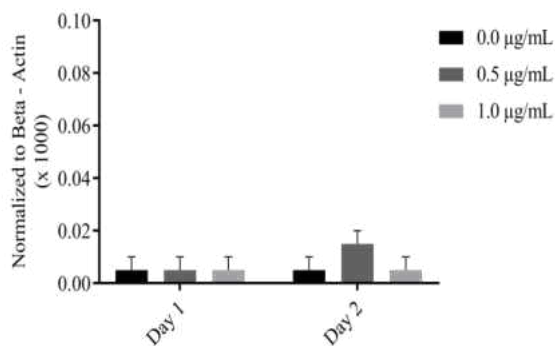
FIGURE III-23, B: Expression of MT-3 in As #1 Transformed Cell Line exposed to Cisplatin
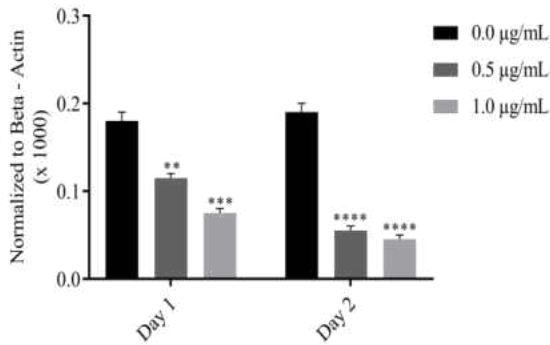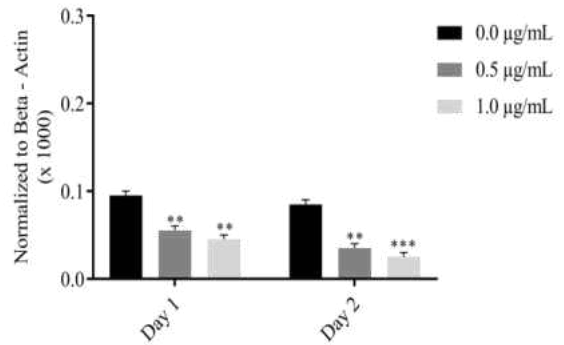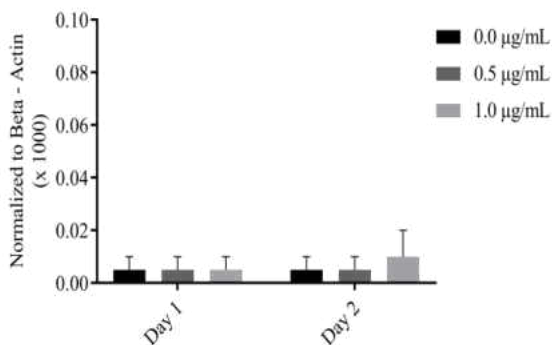

FIGURE III-23, C: Expression of MT-3 in As #5 Transformed Cell Line exposed to Cisplatin
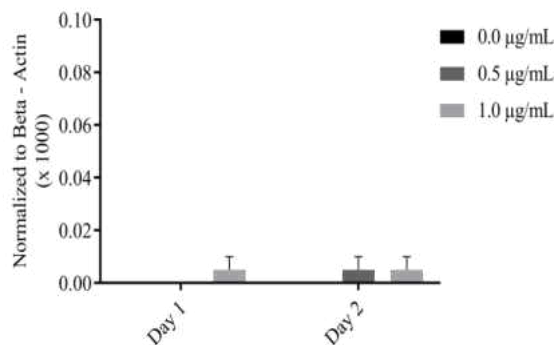
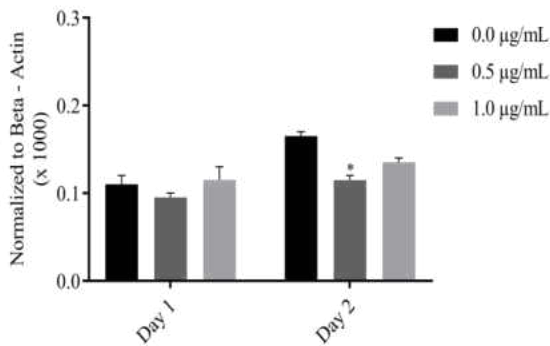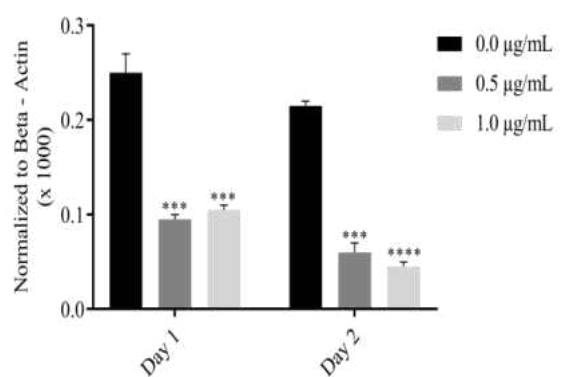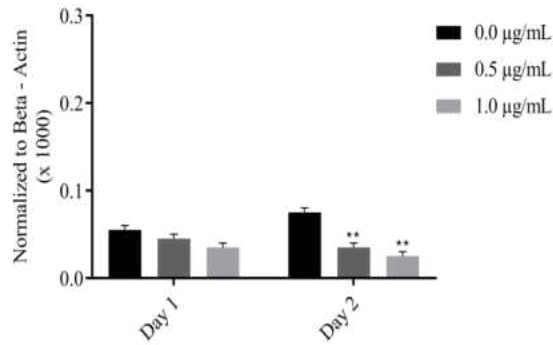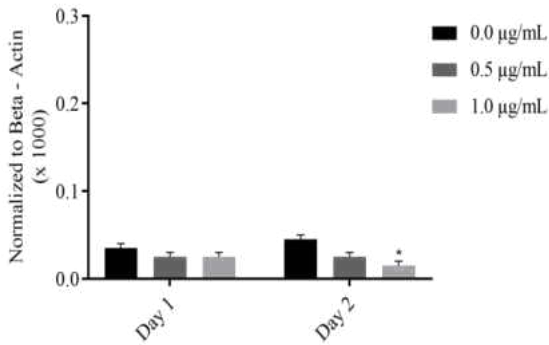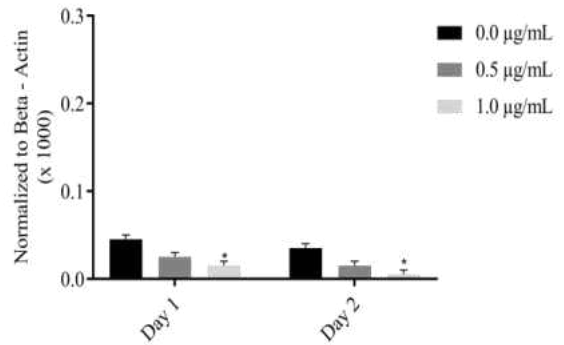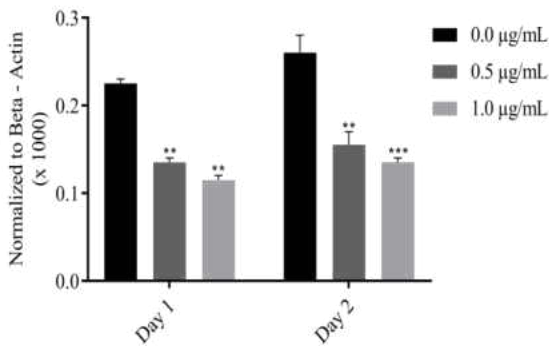**FIGURE III-23, D:** Expression of MT-3 in Cd #1 Transformed Cell Line exposed to Cisplatin
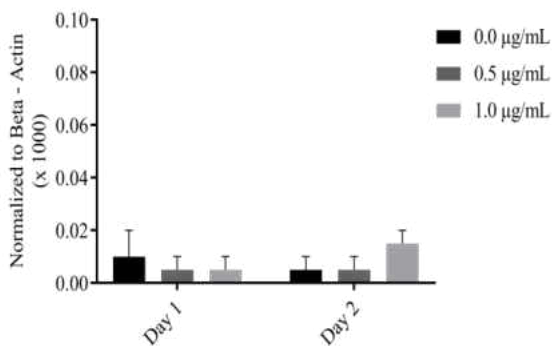
FIGURE III-23, E: Expression of MT-3 in Cd #4 Transformed Cell Line exposed to Cisplatin

60
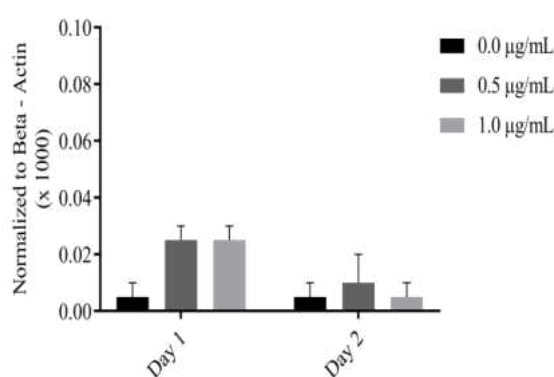
Expression of Metallothioneins exposed to Cisplatin Western Blot Analysis.

Western blot analysis is an important technique used in cell and molecular biology. Through western blot analysis, scientists are able to identify specific protein concentrations from complex mixtures. This technique uses three elements to identify protein concertation, first separation by size, second transfer to a solid support, and third proper target antibodies. In this project the western blots were probed for MT isoforms 1/2 (E9 Clone) followed by β-Actin as a control. MT isoforms 1/2 is a monoclonal antibody that encompasses all of the MT isoform 1 and MT isoform 2. The antibody was purchased from DAKO. More specific details described in the Methods and Materials.

The cells were subjected to an acute cisplatin exposure before being harvested. More specific details on the acute cisplatin exposure as described in the Methods and Materials. The cells lines that were tested were As #1, As #5, Cd #1, and Cd #4, along with the Parent UROtsa cell line. There is not a single real time RT-qPCR graph that aligns with each western blot analysis due to the fact that the western blot analysis antibody encompasses all of the MT isoform 1 and MT isoform 2. On the other hand, the real time RT-qPCR primers that were used were MT isoform specific, therefore we have five real time RT-qPCR graphs that all align with each western blot analysis.

Western blot analysis performed on the Parent UROtsa cell line showed that there was a decrease in the expression levels of MT protein when the cells were exposed to cisplatin. This decrease was visible at 0.5 µg/mL and 1.0 µg/mL doses of cisplatin at both Day #1 and Day #2 (Figure III-24). The cells were striped and re-probed for β-Actin.

The expression of MT protein was also determined for the As^{3+}-transformed cell lines, As #1 and As #5. The data showed that there was an increase in the expression of MT protein in As #1 at 0.5 µg/mL and 1.0 µg/mL doses of cisplatin. However, at Day #2, the expression was still increased in the cells exposed to 0.5 µg/mL of cisplatin. Additionally, the cells that were exposed to 1.0 µg/mL of cisplatin had expression levels similar to the untreated control cells (Figure III-25). For As #5, there was an increase in expression of MT protein on Day #1 at 0.5 µg/mL. The increased expression as a result to the exposure to cisplatin remained elevated both days of the acute cisplatin exposure (Figure III-26). The cells were striped and re-probed for β-Actin.

The effect of cisplatin exposure on MT levels were also determined for the Cd^{2+}-transformed cell lines, Cd #1 and Cd #4. As seen in Figure III-27, there was a decrease in expression of MT when the cells were exposed to 0.5 µg/mL and 1.0 µg/mL of cisplatin on Day #1 and Day #2. The expression of MT protein in Cd #4 was opposite to what was seen in Cd #1. The exposed cells showed an increase in expression at 0.5 µg/mL and 1.0 µg/mL on Day #1, as well as, Day #2 (Figure III-28). The cells were striped and re-probed for β-Actin.

Figure III-24. Expression of MT-1/2 in the Parent UROtsa Cells exposed to Cisplatin.

The Western blots analysis were probed for MT isoforms 1/2 (E9 Clone), then striped and re-probed for β-Actin as a control. MT isoforms 1/2 is a monoclonal antibody that encompasses all of the MT isoform 1 and MT isoform 2. The #'s identify the independent cells lines that were isolated by the exposure of UROtsa cells to either As^{3+} or Cd^{2+}. These numbers are consistent identifiers throughout the paper.

MT-1/2, E9 15 kD

B-Actin 42 kD

0.0 µg/mL 0.5 µg/mL 1.0 µg/mL 0.0 µg/mL 0.5 µg/mL 1.0 µg/mL

Day #1   Day #2
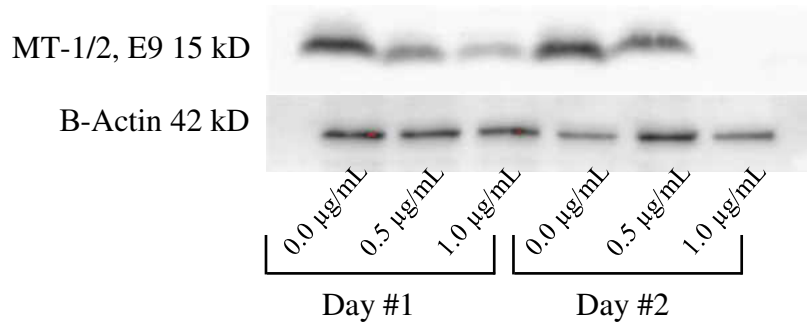
Figure III-25. Expression of MT-1/2 in As #1 Cells exposed to Cisplatin.

The Western blots analysis were probed for MT isoforms 1/2 (E9 Clone), then striped and re-probed for β-Actin as a control. MT isoforms 1/2 is a monoclonal antibody that encompasses all of the MT isoform 1 and MT isoform 2. The #'s identify the independent cells lines that were isolated by the exposure of UROtsa cells to either As^{3+} or Cd^{2+}. These numbers are consistent identifiers throughout the paper.

MT-1/2, E9 15 kD

B-Actin 42 kD

0.0 μg/mL   0.5 μg/mL   1.0 μg/mL   0.0 μg/mL   0.5 μg/mL   1.0 μg/mL

Day #1   Day #2
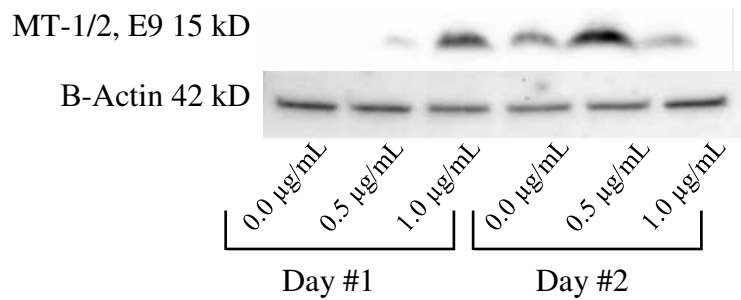
Figure III-26. Expression of MT-1/2 in As #5 Cells exposed to Cisplatin.

The Western blots analysis were probed for MT isoforms 1/2 (E9 Clone), then striped and re-probed for β-Actin as a control. MT isoforms 1/2 is a monoclonal antibody that encompasses all of the MT isoform 1 and MT isoform 2. The #'s identify the independent cells lines that were isolated by the exposure of UROtsa cells to either As^{3+} or Cd^{2+}. These numbers are consistent identifiers throughout the paper.

MT-1/2, E9 15 kD

B-Actin 42 kD

0.0 µg/mL 0.5 µg/mL 1.0 µg/mL   0.0 µg/mL 0.5 µg/mL 1.0 µg/mL

Day #1   Day #2
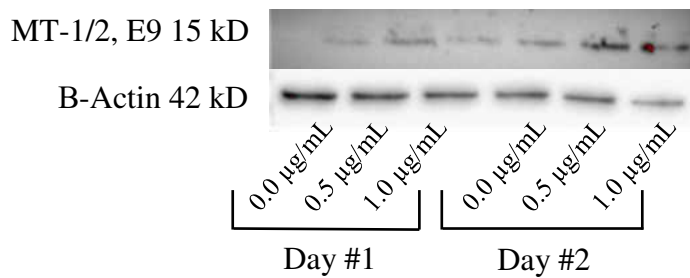
Figure III-27. Expression of MT-1/2 in Cd #1 Cells exposed to Cisplatin.

The Western blots analysis were probed for MT isoforms 1/2 (E9 Clone), then striped and re-probed for β-Actin as a control. MT isoforms 1/2 is a monoclonal antibody that encompasses all of the MT isoform 1 and MT isoform 2. The #'s identify the independent cells lines that were isolated by the exposure of UROtsa cells to either As^{3+} or Cd^{2+}. These numbers are consistent identifiers throughout the paper.

MT-1/2, E9 15 kD

B-Actin 42 kD

0.0 µg/mL   0.5 µg/mL   1.0 µg/mL   0.0 µg/mL   0.5 µg/mL   1.0 µg/mL

Day #1   Day #2
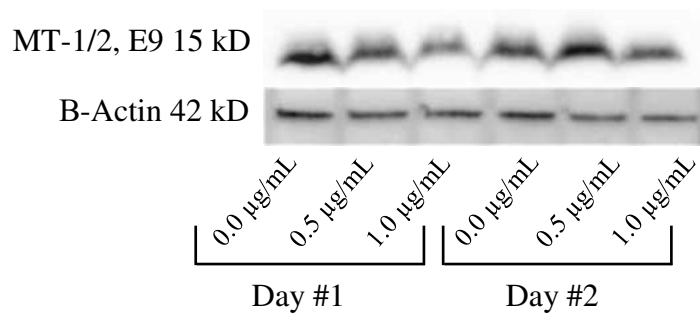
Figure III-28. Expression of MT-1/2 in Cd #4 Cells exposed to Cisplatin.

The Western blots analysis were probed for MT isoforms 1/2 (E9 Clone), then striped and re-probed for β-Actin as a control. MT isoforms 1/2 is a monoclonal antibody that encompasses all of the MT isoform 1 and MT isoform 2. The #'s identify the independent cells lines that were isolated by the exposure of UROtsa cells to either As^{3+} or Cd^{2+}. These numbers are consistent identifiers throughout the paper.
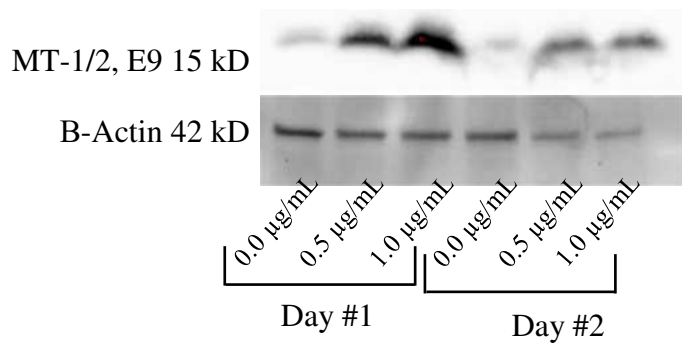
CHAPTER IV.

DISCUSSION.

Metallothionein Expression Levels.

This study was motivated by the recent increase in literature referencing an *in-vivo* relationship between resistance to cisplatin and MT isoform expression levels. MT are a well-known and highly studied cysteine-rich, low molecular weight family of intracellular proteins that bind to heavy metals with high affinity (Andrews, 2000). Human bladder cancer was the first cancer that found industrial carcinomas were determined to play a major role in disease causation (Zhou, et al., 2006). This was observed by Rehn in 1895 (Dietrich & Dietrich, 2001). He suggested there was a link between exposure to aromatic amines and development of bladder cancer in factory workers (Rehn, 1895). This now extends to the present and confirms that exposure to the human carcinogens As^{+3} and Cd^{+2} occurs via environmental exposure, cigarette smoking, industrialization, and contaminated water sources (Somji, et al., 2008).

To further study the effects of As^{+3} and Cd^{+2} our laboratory transformed the UROtsa cell line with them. The UROtsa cell morphology aligns with primary urothelial cells growing in tightly packed colonies allowing investigation into the preliminary phase of development, making it an ideal cell line to study early bladder cancer (Rossi, et al., 2001). Our laboratory has exposed the immortalized UROtsa cell line to As^{3+} or Cd^{2+} in order to establish an *in-vitro* cell culture model that is representative of the mechanisms involved in early bladder cancer. UROtsa cells can serve as a valuable adjunct for studying the human urothelium in general and the stress response in particular (Rossi, et al., 2001). Our laboratory has even further characterized the As^{3+} -and Cd^{2+} -transformed cell lines to express genes similar to the basal subtype of muscle invasive bladder cancer (Hoggarth, et al., 2018)

The first goal of this study is to determine the expression level of six MT isoforms in the Parent UROtsa cell line and the independently derived As^{+3} -and Cd^{+2} -transformed cell lines. To assess the expression of the MT isoforms, real time RT-qPCR analysis was conducted. Our real time RT-qPCR data demonstrated that the MT isoforms showed a decreased expressed in the UROtsa As^{3+} -and Cd^{2+} -transformed cell lines compared to the Parent UROtsa with a few exceptions. IHC analysis of the tumor transplants generated by the subcutaneous injection of the transformed cell lines into immune-compromised mice showed that there is moderate or weak-to-moderate staining of MT isoforms 1/2 in the subcutaneous tumors. However, the staining for MT isoform 3 was strong and diffuse with weaker staining in the less differentiated peripheral cells. This data contradicts the *in-vitro* data where MT isoform 3 is not expressed in the transformed cell lines. It seems that the expression of MT isoform 3 is turned off *in-vitro* and *in-vivo* there is increase expression of

MT isoform 3. This agrees with other studies which have shown an increase expression of MT isoform 3 in human bladder tumors. MT isoform 3 is known to decrease the growth rate of cells and it is possible that the cells *in-vitro* are tuning off the expression since it inhibits the growth of the cells.

Decreased expression of the MT isoforms 1/2 isoforms in the As^{3+}-and Cd^{2+}-transformed cell lines can be explained by several properties that have been cited within the literature. As described previously, MT normal role provides minimal detoxification by uptake, transport, and regulation of metals in cellular biological systems and tissues (Nagel and Vallee, 1995). However, each of the MT isoforms are regulated independently of each other and can have unique expressional changes from the presence of metals, stress hormones, cytokines, reactive oxygen species (ROS), and chemicals (Laukens, 2009). The literature has shown that ROS generated during the inflammatory response may activate or repress MT expression, as well as, specific metal response elements associated with second-messenger protein kinase pathways (Ren and Smith, 1995). It is possible that exposure to the heavy metals during the transformation process disrupted redox homeostasis. Under physiologic conditions, the balance between generation and elimination of ROS/RNS maintains the proper function of redox-sensitive signaling proteins (Trachootham, Lu, Ogasawara, Rivera-Del Valle, & Huang, 2008). Normally, the redox homeostasis ensures that the cells respond properly to endogenous and exogenous stimuli. However, when the redox homeostasis is disturbed, oxidative stress may lead to aberrant cell death (Trachootham, Lu, Ogasawara, Rivera-Del Valle, & Huang, 2008). This may explain why we see a decrease expression of the six MT isoforms in the As^{3+}-and Cd^{2+}-transformed cell

lines but not in the Parent UROtsa cell line. ROS and cellular oxidant stress are known

regulators of cancer cells (Qiu, et al., 2015).

Metallothionein Expression Levels in Cells exposed to Cisplatin.

Cisplatin is a platinum complex that consists of two carrier ligands of ammonia and

two leaving groups of chloride. Literature suggest that there is a growing number of patients

that are developing a resistance to cisplatin (Köberle and Piee-Staffa, 2011). MT

overexpression may predict unfavorable survival in bladder cancer patients in those treated

with cisplatin chemotherapy (Wulfing, et. al., 2007). It is estimated that about 68.0%

of bladder tumors will respond to cisplatin-based chemotherapy but only 30.0% will have a

durable response (Wood, Klein, Fair, & Chaganti, 1993). In a human study that focused on

TCC of the bladder with IHC methods showed all of the tumors stained positive for MT. The

MT staining was localized almost exclusively to the cytoplasm (Bahnason, et. al., 1991).

Other patient studies also demonstrate the survival rate is significantly poorer if tumors are

expressing high levels MT (Wulfing, et. al., 2007). Thus, due to the increases resistance that

is being developed against cisplatin, the effectiveness of the drug is decreasing resulting in a

higher recurrence rate.

The second goal of this study is to determine the expression levels of MT in the

Parent UROtsa, two As^{+3} –and two Cd^{+2} -transformed cell lines when they are acutely

exposed to various concentrations of the chemotherapy drug, cisplatin. The real time RT-

qPCR analysis consisted of mRNA levels that were treated with either 0.0 µg/mL (control),

71

0.5 µg/mL, or 1.0 µg/mL of cisplatin over a two-day (48-hour) treatment period. Overall, the results showed that the expression of MT decreased in response to cisplatin. Western blot analysis was also performed to determine the total levels of MT isoforms 1/2. The expression levels of the MT isoforms 1/2 protein varied between cell lines, however treatment with cisplatin showed a decrease in the level of total MT isoforms 1/2 protein. This suggests that it is possible that the cancer cells may develop a mechanism to decrease MT levels in response to cisplatin exposure as this may aid in the growth and metastasis of the tumor. The mechanism by which the malignant cells decrease the expression of MT isoform 1/2 in response to cisplatin is not known at this time.

The mechanism by which bladder cancer develops a resistance to the chemotherapy drug cisplatin is not fully known, however literature suggests that an over expression of MT play a major role (Hagrman, Goodisman, Dabrowiak, & Souid, 2003). Due to the fact that cisplatin is a platinum complex it is suspected that it is being regulated out by the normal function of the MT isoforms (Gelasco & Lippard, 1998). Therefore the overexpression of MT seen in the *in-vivo* tumors correlates to the resistance of the drug in patients. Our results show that there was a decreased expression of the six MT isoforms in the As^{3+}-and Cd^{2+}-transformed cell lines. This decrease in MT expression may disrupt the normal cellular redox within the cells, thus promoting the transformation process.

Significance.

The overall goal of this study was to determine if the expression levels of the six MT isoforms corresponds to resistance in patients to treatment with cisplatin. The expectation that there is a relationship was based on several factors shown within literature that defines the relationship between MT expression and cisplatin resistance *in-vivo*. Our *in-vitro* results show that were exposure to As^{3+} or Cd^{2+} decreases the expression of MT. This decrease in MT expression may disrupt the normal cellular redox within the cells, thus promoting the transformation process (Trachootham, Lu, Ogasawara, Rivera-Del Valle, & Huang, 2008). Normally, the redox homeostasis ensures that the cells respond properly to endogenous and exogenous stimuli. However, in this case the disruption may mean the decreased expression levels of the MT isoforms will be less likely to interfere with the cisplatin. This would mean that the patient would have a reduced chance of developing resistance to cisplatin and a higher patient prognosis. In addition, exposure to cisplatin in the presence of reduced of MT expression may have implications in the treatment of bladder cancer with this drug.

Authenticity Statement.

To our knowledge no studies have been done to date to evaluate the six MT isoforms used throughout this project to determine the expression in correlation to the resistance of cisplatin in the Parent UROtsa and the As^{3+} -and Cd^{2+} -transformed cell lines. In this study, analyses were performed on the immortalized UROtsa cell lines, As^{3+} -and Cd^{2+}-transformed cell lines and on mouse heterotransplant tumors samples to evaluate the expression of six MT isoforms. Further analyses were performed on the UROtsa cell lines, two As^{3+} -and two Cd^{2+}-transformed cell lines that were acutely exposed to cisplatin. The overall goal was to attempt to better characterize the mechanisms in play between the MT and the development to cisplatin in bladder cancer. In many studies, there are evidence suggesting that increased expression of MT correlates to cisplatin resistance and poor patient prognosis, however further studies are necessary to correlate the data with clinical outcomes.

APPENDICES

APPENDIX A.

Abbreviations.

ACS	American Cancer Association
ANOVA	One-Way Analysis of Variance
As^{3+}	Arsenite
BCA	Bicinchoninic Acid Assay
BCA	Bicinchoninic Acid Assay
BFD	Blackfoot Disease
BFD	Blackfoot Disease
BSA	Bovine Serum Albumin
C	Carbon
Cd^{2+}	Cadmium
CDC	Center for Disease Control and Prevention
$CdCl_2$	Cadmium Chloride
cDNA	Complementary DNA
CERCLA	Comprehensive Environmental Response, Compensation, and Liability Act

Cisplatin	Cis-diamminediechloroplatinum(II), CDDP
CNS	Central Nervous System
Co	Cobalt
CO_2	Carbon Dioxide
Cu	Copper
DAB	3,3'-Diaminobenzidine
DMEM	Dulbecco's Modified Eagle Medium
DNA	Deoxynucleic Acid
FCS	Fetal Calf Serum
Fe	Iron
GHS	Glutathione
H	Hydrogen
H_2O	Water
Hg	Mercury
IARC	International Agency for Research on Cancer
IHC	Immunohistochemistry
MCL	Maximum Containment Level
mRNA	Messenger Ribonucleic Acid
MT	Metallothionein
MTT	3-(4,5-Dimethylthiazol-2-yl)-2,5-Diphenyltetrazolium Bromidefor
N	Nitrogen
Na	Sodium
$NaAsO_2$	Sodium Arsenite

NaCl	Sodium Chloride
NH_3	Ammonia
Ni	Nickel
NTP	National Toxicology Program
O	Oxygen
Pb	Lead
PBS	Phosphate Buffered Saline
PMSF	Phenylmethane Sulfonyl Fluoride
Pt	Platinum
PVD	Peripheral Vascular Disease
PVD	Peripheral Vascular Disease
PVDF	Polyvinylidene Difluoride
rcf	Relative Centrifuge Force
RIPA	Radioimmunoprecipitation Assay Buffer
RT-qPCR	Real-Time Quantitative Polymerase Chain Reaction
S^{2-}	Sulfide
Se	Selenium
SEM	Standard Error of the Mean
SV40	Simian Vacuolating Virus 40 or *Simian Virus 40*
T-antigen	Tumor Antigen
TBS	Tris-Buffered Saline
TBS-T	TBS-Tween
TCC	Transitional Cell Carcinomas

Zn	Zinc
β-Actin	Beta-Actin
β-Mercaptoethanol	Beta-Mercaptoethanol

Units of Measurement.

AMP   Ampere

cm^2 Centimeters Squared

kDa   KiloDalton

L   Liter

mL   Milliliter (10^{-3} Liter)

mM   Millimolar (10^{-3} Mole/Liter)

mm   Millimeter (10^{-3} Meter)

rcf   Relative Centrifugal Force

V   Volts

˚C   Degrees Celsius

μg   Microgram (10^{-9} Gram)

μM   Micromolar (10^{-6} Mole/Liter)

μm   Micrometer (10^{-6} Meter)

APPENDIX B.

Buffers and Solution Recipes.

20/12 Media

> 250.0 mL DMEM (Sigma Aldrich #D5523-10)
>
> 250.0 mL Nutrient Mixture F12 Ham (Sigma Aldrich #N6760-10)
>
> 5.0 mL L.Glutamine (Gibco #25030-81)
>
> 5.0 mL Recombinant Human E.G.F. Lyophilized (Sigma #PHG0311)
>
> 0.5 mL ITS Premix Universal Culture Supplement (Corning #354350)
>
> 0.5 mL T3 (Sigma #T6397)
>
> 0.5 mL HC (Gibco #EL0013)

Dulbecco's Modified Eagle Medium (DMEM)

> 4945.0 mL Milli Q Water
>
> 5.0 Bottles DME Powder (Sigma #D5523-10)
>
> 50.0 mL Penicillin-Streptomycin (Pen-Strep) (Gibco #15140-122)
>
> 5.0 m L FungiZone (Gibco #15920-018)
>
> 18.5 g Na-Bicarbonate (Fisher Chemicals #BP328-500)

F-12 Media

      4945.0 mL Milli Q Water

      1.0 Bottle Nutrient Mixture F-12 HAM (Sigma #N6760-10)

      5.0 mL FungiZone (Gibco #15920-018)

      50.0 m L Penicillin-Streptomycin (Pen-Strep) (Gibco #15140-122)

      5.88 g Na-Bicarbonate (Fisher Chemicals #BP328-500)

Phosphate Buffered Saline (PBS)

      5.0 L Milli Q Water

      42.5 g NaCl (Sigma Aldrich #S9888-2.5KG)

      0.60 g Na_2HPO_4 (Dibasic) (Fisher Chemicals #BP332-500)

      0.25 g NaH_2PO_4 (Monobasic) (Fisher Chemicals #BP329-500)

0.5X TAE Buffer Molecular Biology Grade

      500.0 mL Milli Q Water

      25.0 mL 10X TBE (BioRad #170-6435)

2.0 % Large Agarose Gel

      65.0 mL 0.5X TBE

      1.3 g Agarose (Fisher BioReagents #BP1356-100)

      1.62 µL Ethidium Bromide (ThermoFisher Scientific #15585011)

2.0 % Small Agarose Gel

      40.0 mL 0.5X TBE

      0.4 g Agarose (Fisher BioReagents #BP1356-100)

      1.0 µL Ethidium Bromide (ThermoFisher Scientific #15585011)

1X Tris/Glycine/SDS Solution (Running Buffer)

       675.0 mL Milli Q Water

       75.0 mL 10X Tris/Glycine/SDS Solution (BioRad #161-0732)

1X Tris Buffered Saline (TBS)

       450.0 mL Milli Q Water

       50.0 mL 10X TBS (BioRad #170-6435)

1X Tris Buffered Saline - 1.0 % Tween (TBST)

       450.0 mL Milli Q Water

       50.0 mL 10X TBS (BioRad #170-6435)

       5.0 mL Tween (Sigma #P1379-500)

APPENDIX C.

Real Time RT-qPCR and C_t Cycle Introduction.

The general reaction system of conventional PCR is the same for real-time PCR, the only difference is that the accumulation of product is monitored within the reaction tube at the end of each PCR cycle. The DNA is detached by fluorescence of the intercalating dye, such as SYBR green. Much like ethidium bromide, when this dye intercalates with double stranded DNA the intensity of the fluorescence is dramatically increased. Primers attach to the ends of the PCR product. The upper primer (sense primer) has the same sequences as that found in the RNA and the lower primer (antisense primer) or downstream primer has a sequence that is the reverse complement of the corresponding sequences in the RNA.

Amplification should be 90% or better in an optimized reaction. This means that the amount of DNA should nearly double at every cycle. Mispriming may occur when sequence site in the population of DNA molecules are just a few base pairs off from the primer sequence. One increases the temperature so that only the perfectly matched sequences will be bound by the primer which fixes the misprinting problem. There is a

window of optimal temperature for PCR, where at temperatures above this window, amplification efficiency is falls back off due to lack of priming, and temperatures below this window, results in Mispriming, giving some other amplified products. The size of this window is determined by the differences in the sequence at the potential primer binding sites. Large sequence differences should yield a large range of optimal PCR annealing temperatures. Other factors that determine the temperature of optimal PCR are the length and the GC content of the primers: higher GC content or longer primers will increase primer binding. We have a primer design software called "Oligo" that searches sequences for optimal primers. This program will indicate what temperatures should work, but usually verification by a wet PCR run is required to establish the optimal temperature condition. Sometimes one needs to change the annealing temperature despite all theoretical calculations.

What is it about the real-time techniques that gives it such an advantage? In real-time PCR, the threshold cycle is measured and not the level of product at later stages of amplification. The threshold cycle number is not influences by impurities with the sample unlike most other types of conventional PCR. This has been illustrated by the inform PCR experiment shown below where the same template concentration was amplified in 3 separate wells of the instrument. In this graph, all traces cross the threshold florescence's line at nearly the same place, whereas, at later stages of amplification, the traces diverge from each other. It is this quality of technique, measuring threshold cycle number that allows one to make standard curves. In conventional PCR, standards cannot be run for the amplification efficiency in the later stages of CR slightly different among the individual sample tubes.

A typical profile of amplifications: it looks like a sigmoid curve. It starts with increasing slope which represents the exponential phase of the curve, followed by a linear phase where amplification efficiency is starting to fall off, and finally a gradual leveling off to a plateau phase. Most of the time when this is published, the fluorescence is plotted on a log graph which makes it look more impressive. Not that all the samples with higher amounts of template are amplified first.

How is a standard curve generated? Quantitated amounts of template, serially diluted are added to each tube and the threshold cycle (C_t) number is measured. For the standard curve, the threshold cycle number is plotted against the log of the template input (see figure below). The slope of the standard curve is negative, and the amplification efficiency can be calculated from this. Efficiency (expressed as a decimal, 0.1 equals 100%) = [10E (-1/slope)]-1. The efficiency is 100% when the slope is -3.32. The slope expresses the fact that it takes 3.32 more cycles of PCR to reach the threshold when the samples is diluted 1-10 and amplification is 100%. Perfect amplification efficiency indicates that the product amount will double at each cycle, therefor at 3 cycles the product increase 9-fold, at 4 cycles, 16-fold, and 10-fold in calculated to by a 3.32 cycles. In the real world efficiency is often less due to random error and impurities, and since the slope is essentially calculated by the linear regression using the least-squares approach, the slope can occasionally be less than -3.32 just from random errors in producing standard curves. This means that greater than 100% is also possible. Generally when things are working 80 to 120% efficiencies can be seen and often it can be limited to the range of 90 to 110 %. Much higher efficiencies are often caused by contamination where the lower concentration standards have reach a limited threshold cycle (further dilution

86

does not yield a higher threshold cycle number). This simple bends the curve to a flatter

configuration leading to a less negative slope in the curve. This is fixed by simply

deleting the standard from the curve.

BIBLIOGRAPHY

2007 CERCLA Priority List of Hazardous Substances. (2018, December). Retrieved from

Centers for Disease Control and Prevention:

https://www.atsdr.cdc.gov/spl/previous/07list.html

Andersson, K. E., & Arner, A. (2004). Urinary Bladder Contraction and Relaxation:

Physiology and Pathophysiology. *American Physiological Society*, 84(3):935-86.

Arsenic. (2018, December). Retrieved from World Health Organization:

http://www.who.int/news-room/fact-sheets/detail/arsenic

ATSDR. (2007). *Toxicological Profile for Arsenic. U.S. Department of Health and Human*

Services, Public Health Service. Atlanta, GA. Retrieved from

http://dx.doi.org/10.1155/2013/286524

ATSDR. (2012, December). *Toxicological Profile for Cadmium. U.S. Department of Health*

and Human Services, Public Health Service. Atlanta, GA. Retrieved from

http://www.atsdr.cdc.gov/toxprofiles/tp5.pdf\nhttp://www.ncbi.nlm.nih.gov/books/N

BK158845/

Bahnason, R. R., Banner, B. F., Ernstoff, M. S., Lazo, J. S., Cherian, M. G., Banerjee, D., & Chin, J. L. (1991). Immunohistochemical localization of Metallothionein in Transitional Cell Carcinoma of the Bladder. *The Journal of Urology*, 146(6):1518-20.

Bhattacharya, P., Welch, A. H., Stollenwerk, K. G., McLaughlin, M. J., Bundschuh, J., & Panaullah, G. (2007). Arsenic in the Environment: Biology and Chemistry. *The Science of the Total environment*, 379(2-3):109-20.

Biggers, A., & Paddock, M. (2018, December). *What is Arsenic Poisoning?* Retrieved from Medical News Today: https://www.medicalnewstoday.com/articles/241860.php

Bladder Cancer Statistics. (2018, December). Retrieved from American Institute for Cancer research: https://www.wcrf.org/dietandcancer/cancer-trends/bladder-cancer-statistics

Chabin-Brion, K., Marceiller, J., Perez, F., Settegrana, C., Drechou, A., Durand, G., & Pous, C. (2001). The Golgi Complex is a Microtubule-Organizing Organelle. *Molecular Biology of the Cell*, 12(7):2047-60.

Chiou, H., Hsueh, Y., Liaw, K., Horng, S., Chiang, M., Pu, Y., & Chen, C. (1995). Incidence of internal Cancers and Ingested Inorganic Arsenic: a Seven-Year follow-up Study in Taiwan. *Cancer Research*, 55(6):1296-300.

Choudhury, H., Harvey, T., Thayer, Thayer, W. C., Lockwood, T. F., Stieteler, W. M., . . . Diamond, G. L. (2001). Urinary Cadmium Elimination as a Biomarker of Exposure for Evaluating a Cadmium Dietary Exposure--Biokinetics Model. *Journal of Toxicology and Environmental Health*, 63(5):321-50.

Cisplatin. (2018, December). Retrieved from Chemocare:

http://chemocare.com/chemotherapy/drug-info/cisplatin.aspx

Dietrich, H. G., & Dietrich, B. (2001). Ludwig Rehn (1849-1930)--Pioneering findings on

the Aetiology of Bladder Tumours. *World Journal of Urology*, 19(2):151-3.

Ferguson, L. R., & Baguley, B. C. (1994). Mutagenicity of Anticancer Drugs that inhibit

Topoisomerase Enzymes. *Science Direct*, 355(1-2):91-101.

Freedman, N. D., Silverman, D. T., Hollenbeck, A. R., Schatzkin, A., & Abnet, C. C. (2011).

Association between Smoking And Risk of Bladder Cancer among Men and Women.

JAMA, 306(7):737-45.

Garrett, S. H., Park, S., Sens, M. A., Somji, S., Singh, R. K., Namburi, V. B., & Sens, D. A.

(2005). Expression of Metallothoinein Isoform 3 Is Restricted at the Post-

Transcriptional Level in Human Bladder Epithelial Cells. *Toxicological Sciences*,

87(1):66-74.

Garrett, S. H., Somji, S., Todd, J. H., Sens, D. A., Lamm, D. L., & Sens, M. A. (1999).

Metallothionein isoform Gene Expression in four Human Bladder Cancer Cell.

Klasseen C.D. Metallothionein IV. Advances in Life Sceinces, 607-612.

https://doi.org/10.1007/978-3-0348-8847-9_91.

Gelasco, A., & Lippard, S. J. (1998). NMR Solution Structure of a DNA Dodecamer Duplex

Containing a cis-Diammineplatinum(II) d(GpG) Intrastrand Cross-Link, the Major

Adduct of the Anticancer Drug Cisplatin. *Biochemistry*, 37(26):9230–39.

Gonzalez, V. W., Fuertes, M. A., Alonso, C., & Perez, J. M. (2001). Is cisplatin-induced cell death always produced by Apoptosis? *American Society for Pharmacology and Experimental Therapeutics*, 59(4):657-63.

Hagrman, D., Goodisman, J., Dabrowiak, J. C., & Souid, A. K. (2003). Kinetic Study on the Reaction of cisplatin with Metallothionein. *Drug Metabolism and Disposition : The Biological fate of Chemicals*, 31(7):916-23.

Hamer, D. (1986). Metallothioneins. *Annual Review of Biochemistry*, 55(1):913-51.

Hoggarth, Z. E., Osowski, D. B., Freeberg, B. A., Garrett, S. H., Sens, D. A., Sens, M. A., Somji, S. (2018). The Urothelial Cell Line UROtsa transformed by Arsenite and Cadmium displayed basal characteristics associated with Muscle Invasive Urothelial Cancers. *PLOS ONE*.

Hueper, W., Wiley, F., & Wolfe, H. (1938). Experimental production of Bladder Tumors in Dogs by Administration of Beta-aphthylamine. *Journal of Industrial Hygeine and Toxicology*, 20:46–84.

Inaba, T., Kobayashi, E., Suwazono, Y., Uetani, M., Oishi, M., Nakagawa, H., & Nogawa, K. (2005). Estimation of cumulative Cadmium intake causing Itai-itai Disease. *Toxicology Letters*, 159(2):192–201.

Inbred & outbred nude mice. (2018, December). Retrieved from The Jackson Laboratory: https://www.jax.org/jax-mice-and-services/find-and-order-jax-mice/most-popular-jax-mice-strains/nude-mice

Isani, G., & Carpene, E. (2014). Metallothioneins, Unconventional Proteins from Unconventional Animals: A Long Journey from Nematodes to Mammals. *Biomolecules*, 4(2):435–457.

Iverson, C. (2018, December). *Adult Human Urinary System.* Web.

Jacobs, B. L., Lee, C. T., & Montie, J. E. (2010). Bladder Cancer in 2010: How far have we come? *CA: A Cancer Journal for Clinicians*, 60(4):244-72.

Jang, Y.-C., Somanna, Y., & Kim, H. (2016). Source, Distribution, Toxicity and Remediation of Arsenic in the Environment – A Review. *International Journal of Applied Environmental Sciences*, 11(2):559-81.

Jemal, A., Siegel, R., Xu, J., & Ward, E. (2010). Cancer Statistics, 2010. *CA: A Cancer Journal for Clinicians*, 60(5):277-300.

Johansson, S. L., & Cohen, S. M. (1992). Epidemiology and Etiology of Bladder Cancer. *The Urologic Clinics of North America*, 13(5):291-8.

Keil, D. E., Berger-Ritchie, J., & McMilin, G. A. (2011). Testing for Toxic Elements: A Focus on Arsenic, Cadmium, Lead, and Mercury. *Laboratory Medicine*, 42(12):735-42.

Kellen, E., Zeegers, M. P., Hond, E., & Bunttinx, F. (2007). Blood Cadmium may be associated with Bladder Carcinogenesis: the Belgian case-control study on Bladder Cancer. *Cancer Detection and Prevention*, 31(1):77-82.

Liu, Z. M., Chen, G. G., Shum, C. K., Vlantis, A. C., Cherian, M. G., Koropatnick, J., & Van Hasselt, C. A. (2007). Induction of functional MT1 and MT2 isoforms by Calcium in Anaplastic Thyroid Carcinoma Cells. *Elsevier B.V.*, 581(13):2465-72.

Mandal, B., & Suzuki, K. (2002). Arsenic round the World: a Review. *Talanta*, 58(1):201-35.

Marshall, G., Ferreccio, C., Yuan, Y., Bates, M. N., Steinmause, C., Selvin, S., & Smith, A. (2007). Fifty-year study of Lung and Bladder Cancer mortality in Chile related to Arsenic in Drinking Water. *Journal of the National Cancer Institute*, 99(12):920-8.

Mehus, A. A., Muhonen, W. W., Garrett, S. H., Somji, S., Sens, D. A., & Shabb, J. B. (2014). Quantitation of Human Metallothionein Isoforms: A Family of Small, Highly Conserved, Cysteine-rich Proteins. *The American Society for Biochemistry and Molecular Biology*, 3(4):1020-33.

Midioddi, S., McGuirt, J. P., Sens, M. A., Todd, J. H., & Sens, D. A. (1996). Isoform-specific expression of Metallothionein mRNA in the developing and Adult Human Kidney. *Toxicology Letters*, 85(1):17-27.

NTP. (2011, December). Cadmium and Cadmium Compounds. In U.S. Department of Health and Human Services Public Service (Ed.), National Toxicology Program. Triangle Park, NC.

Qiu, M., Chen, L., Tan, G., Ke, L., Zhang, S., Chen, H., & Liu, J. (2015). A Reactive Oxygen Species activation mechanism contributes to JS-K-induced Apoptosis in Human Bladder Cancer Cells. *Sceintific Reports*, 5(1):15104-16.

Rehn, L. (1985). Blasengeschwuelste bei Fuchsinarbeitern. *Arch Klin*, 50:588-600.

Ross, M. H., & Pawlina, W. (2016). *Histology: A Text and Atlas (6th Edition).* Baltimore,
        MD: Wolters luwer.

Rossi, M. R., Masters, J. R., Park, S., Todd, J. H., Garrett, S. H., Sens, M. A., & Sens, D. A.
        (2001). The Immortalized UROtsa cell line as a potential Cell Culture Model of
        Human Urothelium. *Environmental Health Perspectives*, 109(8):801–8.

Rossi, M. R., Somji, S., Garrett, S. H., Sens, M. A., Nath, J., & Sens, D. A. (2002).
        Expression of hsp 27, hsp 60, hsc 70, and hsp 70 stress response Genes in cultured
        Human Urothelial Cells (UROtsa) exposed to Lethal and Sublethal concentrations of
        Sodium Arsenite. *Environmental Health Perspectives*, 110(12):1225–32.

Satarug, S., & Moore, M. R. (2004). Adverse Health Effects of Chronic exposure to
        Lowlevel Cadmium in Foodstuffs and Cigarette Smoke. *Environmental Health
        Perspectives*, 112(10):1099–1103.

Selius, B. A., & Subedi, R. (2008). Urinary Retention in Adults: Diagnosis and Initial
        Management. *American Family Physician*, 77(5):643-650.

Sens, D. A., Park, S., Gurel, V., Sens, M. A., Garrett, S. H., & Somji, S. (2004). Inorganic
        Cadmium- and Arsenite-induced Malignant Transformation of Human Bladder
        Urothelial Cells. *Toxicological Sciences*, 79(1):56–63.

Sens, D. A., Rossi, M., Park, S., Gurel, V., Nath, J., Garrett, S. H., & Somji, S. (2003).
        Metallothionein Isoform 1 and 2 gene expression in a Human Urothelial Cell Line

(UROtsa) exposed to CdCl2 and NaAsO2. *Journal of Toxicology and Environmental Health*, 66(21):2031–2046.

Sens, M. A., Somji, S., Lamm, D. L., Garrett, S. H., Slovinsky, F., Todd, J. H., & Sens, D. A. (2000). Metallothionein Isoform 3 as a Potential Biomarker for Human Bladder Cancer. *Environmental Health Perspectives*, 108(5):413-8.

Shaloam, D., & Tchounwou, P. B. (2015). Cisplatin in Cancer Therapy: Molecular Mechanisms of Action. *European Journal of Pharmacology*, 740:364-78.

Siemiatycki, J., Dewar, R., & Gerin, M. (1994). Occupational Risk Factors for Bladder Cancer: Results from a Case-Control Study in Montreal, Quebec, Canada. *American journal of epidemiology*, 140(12):1061-80.

Smith, A. H., & Steinmaus, C. M. (2011). Arsenic in Drinking Water. *British Medical Association*, 5;342.

Smith, C., Livingston, S., & Doolittle, D. (1997). An international literature survey of "IARC Group I Carcinogens" reported in mainstream Cigarette Smoke. *Food and Chemical Toxicology*, 35:1107–1130.

Smith, D. A., Jaggi, M., Zhang, W., Galich, A., Du, C., Sterrett, S. P., . . . Balaji, K. C. (2006). Metallothioneins and Resistance to Cisplatin and Radiation in Prostate Cancer. *Urology*, 67(6):1341-7.

Somji, S., Garrett, S. H., Sens, M. A., Gurel, V., & Sens, D. A. (2004). Expression of Metallothionein Isoform 3 (MT-3) Determines the Choice between Apoptotic or

Necrotic Cell Death in Cd+2-Exposed Human Proximal Tubule Cells. *Toxicological Sciences*, 80(2):358-66.

Somji, S., Garrett, S. H., Zhou, X. D., Zheng, Y., Sens, D. A., & Sens, M. A. (2010). Absence of Metallothionein 3 Expression in Breast Cancer is a Rare, But Favorable Marker of Outcome that is Under Epigenetic Control. *Toxicological Enviromental Chemistry*, 92(9):1673-1695.

Steinmaus, C., Ferreccio, C., Acevedo, J., Yuan, Y., Liaw, J., Duran, V., . . . Smith, A. H. (2014). Increased Lung and Bladder Cancer Incidence In Adults After In Utero and Early-Life Arsenic Exposure. *Cancer Epidemiol Biomarkers Prev*, 23(8):1529-38.

Steinmaus, C., Ferreccio, C., Romo, J. A., Yuan, Y., Cortes, S., Marshall, G., & Smith, A. H. (2013). Drinking water arsenic in northern chile: high cancer risks 40 years after exposure cessation. *Cancer Epidemiology, Biomarkers & Prevention : A Publication of the American Association for Cancer Research, Cosponsored by the American Society of Preventive Oncology*, 22(4):623-30.

Trachootham, D., Lu, W., Ogasawara, M. A., Rivera-Del Valle, N., & Huang, P. (2008). Redox Regulation of Cell Survival. *Antioxidants & Redox Signaling*, 10(8):1343-74.

Tseng, C. H., Huang, Y. K., Chung, C. J., Yang, M. H., Chen, C. J., & Hsueh, Y. M. (2005). Arsenic exposure, urinary arsenic speciation, and peripheral vascular disease in blackfoot disease-hyperendemic villages in Taiwan. *Toxicology and applied pharmacology*, 206(3):299-308.

Tseng, W. P. (1977). Effects and dose response relationships of skin cancer and blackfoot disease with arsenic. *Environmental Health Perspectives*, 19:109-19.

Urinary Retention. (2018, December). Retrieved from National Institute of Diabetes and

    Digestive and Kidney Diseases: https://www.niddk.nih.gov/health-

    information/urologic-diseases/urinary-retention

Wood , D. P., Klein, E., Fair , W. R., & Chaganti, R. S. (1993). Metallothionein gene

    expression in bladder cancer exposed to cisplatin. *Modern Pathology: United States*

    and Canadian Academy of Pathology, 6(1):33-5.

Wulfing, C., Van Ahlen, H., Eltze, E., Piechota, H., Hertle, L., & Schmid, K. W. (2007).

    Metallothionein in bladder cancer: correlation of overexpression with poor outcome

    after chemotherapy. *Urological Research Society*, 25(2):199-205.

Yeung, C., Dinh, T., & Lee, J. (2014). The Health Economics of Bladder Cancer: An updated

    Review of the Published Literature. *PharmacoEconomics*, 32(11):1093-104.

Zeegers, M., Tan, F., Dorant, E., & Van Den Brandt, P. (2000). The impact of characteristics

    of cigarette smoking on urinary tract cancer risk: a meta-analysis of epidemiologic

    studies. *Cancer*, 89(3):630-9.

Zhou, X. D., Sens , D. A., Sens, M. A., Namburi, V. B., Singh, R. K., Garrett, S. H., &

    Somji, S. (2006). Metallothionein-1 and -2 Expression in Cadmium- or Arsenic-

    Derived. *Toxicological Sciences*, 93(2):322–30.

Zimmermann, K. A. (2018, December). *Urinary System: Facts, Functions & Diseases*.

    Retrieved from Live Science: https://www.livescience.com/27012-urinary-

    system.html